ADDIS ABABA UNIVERSITY

COLLEGE OF HEALTH SCIENCES

SCHOOL OF PHARMACY

DEPARTMENT OF PHARMACEUTICS AND SOCIAL PHARMACY

Preparation, Characterization of Cellulose Acetate from Cotton Linter and Evaluation as a Sustained Release Excipient in Tablet Formulations

Melaku Teshome (B. Pharm)

November, 2021

Addis Ababa

Preparation, Characterization of Cellulose Acetate from Cotton Linter and Evaluation as a Sustained Release Excipient in Tablet Formulations

A Thesis Submitted to Addis Ababa University, College of Health Sciences, School of Pharmacy, Department of Pharmaceutics and Social Pharmacy, in Partial Fulfilment of the Requirements for the Degree of Master of Science in Pharmaceutics

Melaku Teshome (B. Pharm)

Under the Supervision of Prof. Tsige Gebre-Mariam and Dr. Gebre-mariam Birhanu, Department of Pharmaceutics and Social Pharmacy, School of Pharmacy, Addis Ababa University

November, 2021

Addis Ababa

Addis Ababa University School of Graduate Studies

This is to certify that the thesis undertaken by Melaku Teshome, entitled "Preparation, Characterization of Cellulose Acetate from Cotton Linter and Evaluation as a Sustained Release Excipient in Tablet Formulations" and submitted in partial fulfilment of the requirements for the Degree of Master of Science in Pharmaceutics complies with the regulations of the University and meets the accepted standards with respect to originality and quality.

Approved and signed by the Examining Committee:

Name	**Signature**	**Date**
1. Prof. Tsige Gebre-Mariam (Advisor)	_____	_____
2. Dr. Gebre-mariam Birhanu (Advisor)	_____	_____
3. Dr. Getahun Paulos (Examiner)	_____	_____
4. Mr. Fantahun Molla (Examiner)	_____	_____

_____

Head, Department of Pharmaceutics and Social Pharmacy, School of Pharmacy, Addis Ababa University

ACKNOWLEDGMENTS

First of all, I would like to thank almighty God for giving me strength and patience throughout the entire situation and challenge that I faced for successful completion of this study.

I express my deep sense of gratitude to my research supervisors Prof. Tsige Gebre-Mariam and Dr. Gebre-mariam Birhanu for their assistance, invaluable comments, constructive suggestions and excellent supervision throughout my research work. I must also thank them for the encouragement showed towards me, which was very helpful and very much precious.

I am highly thankful to Derry Kebede Cotton Ginning Factory for providing me with cotton linter. I would also like to acknowledge Cadila Pharmaceuticals Ethiopia, PLC for FTIR study; Addis Pharmaceutical Factory (APF), PLC for providing the model drug; East Africa Pharmaceuticals, PLC for allowing me access to tablet compression machine; Ethiopian Public Health Institute for the determination of ash value and Anna University, Tamil Nadu, India for SEM study. My specials thank also goes to Adama Science and Technology University, Department of Materials Science Engineering, for XRD study and Leather Industry Development Institute for thermal analysis.

I would also like to thank Mr. Tesfaye Gabriel for supporting me during my research work and Mr. Fekade Tefera and Mr. Abraham Temesgen for their technical support in the laboratory. I am highly indebted to all other staff members of Department of Pharmaceutics and Social Pharmacy. Furthermore, I would like to thank my family and all my friends who provided me with all-rounded support throughout my study.

Finally, I would like to acknowledge Addis Ababa and Haramaya Universities for sponsoring my postgraduate studies.

ABSTRACT

Cotton linter (CL) is a by-product of the garment industry that is good raw material for cellulose preparation. The aim of this study was to extract and characterize native cellulose and cellulose acetate (CA) from CL and evaluates CA as a sustained release excipient in tablet formulation. In this study, cellulose was extracted by steam explosion method and CA was prepared from the extracted cellulose by using acetic anhydride as acetylating agent and sulphuric acid as a catalyst. Physico-chemical properties of cellulose and CA were characterized. Mechanical properties of plain CA tablets and release profile of theophylline as a model drug were investigated from CA matrix. The cellulose yield from CL on dry weight basis was found to be 78.06%$\pm$1.70, while CA yield from cotton linter cellulose (CLC) was 112.4%$\pm$1.28. The degree of polymerization (DP) of CLC was 472.52$\pm$3.64, while DP of cotton linter cellulose acetate (CLCA) preparations ranged from 148.24$\pm$1.80 - 234.09$\pm$4.12 based on their degree of substitution (DS). The identification of CLCA was confirmed by Fourier transform infrared (FTIR) spectra, while CLC was identified by using chemical test in addition to FTIR. The degree of crystallinity of CLC was 81.59% and those of CLCA with DS 0.83 and DS 2.46 were 57.92% and 33.78%, respectively. Scanning electron microscopy (SEM) of CLC showed fibrous morphology while SEM of CLCA revealed aggregated particles. The CLCA with DS 2.46 exhibited better heat stability than CLC and comparable result with commercial cellulose acetate (CCA). However, CLC exhibited better thermal stability than CLCA having DS 0.83. The CLCA with DS 2.46 exhibited good flow properties making it suitable for direct compression. The release study showed that, matrix tablets of CLCA with DS 2.46 preparations exhibited prolonged disintegration times and retarded *in-vitro* dissolution than tablets prepared with CLCA DS 0.83 and comparable result with CCA. However, CLCA had higher % release of drug as compared to ethyl cellulose (EC) containing formulation. The drug release rate was also prolonged as the percentage of CLCA DS 2.46 increased from 59.5% to 79.5% (w/w). The kinetic study showed that, the formulations are best fitted to the Higuchi's square root kinetic model (R^2 = 0.9862 to 0.9976) indicating the release of drug from the matrix was diffusion based. Therefore, CL could be a potential local source of cellulose while CLCA could be a potential candidate as a sustained release excipient.

Keywords: Cellulose, Cellulose acetate, Cotton linter, Degree of substitution, Sustained release

TABLE OF CONTENTS

LIST OF FIGURES

LIST OF TABLES

ABBREVIATIONS AND ACRONYMS

AGU:	Anhydroglucose Unit
CA:	Cellulose Acetate
CCA:	Commercial Cellulose Acetate
CDA:	Cellulose Diacetate
CI:	Carr's Index
CL:	Cotton Linter
CLC:	Cotton Linter Cellulose
CLCA:	Cotton Linter Cellulose Acetate
COPD:	Chronic Obstructive Pulmonary Disease
CTA:	Cellulose Triacetate
Cuam:	Cuprammonium hydroxide
DP:	Degree of Polymerization
DS:	Degree of Substitution
DSC:	Differential Scanning Calorimetry
DTG:	Derivative Thermo gravimetric
EC:	Ethyl Cellulose
FTIR:	Fourier Transform Infrared
GIT:	Gastrointestinal Tract
HR:	Hausner Ratio
NF:	National Formulary
PFA/PAA:	Performic acid/ peracetic acid
RH:	Relative Humidity
rpm:	Revolution per Minute
SEM:	Scanning Electron Microscope
SR:	Sustained Release
TGA:	Thermogravimetric Analysis
USP:	United States Pharmacopoeia
XRD:	X-Ray Diffraction

1. INTRODUCTION

1.1. Cellulose

Cellulose is the most abundant organic polymer in the world with a total annual biomass production of about 1.5×10^{12} ton. It was discovered in 1838 by, Anselme Payne (Macuja *et al*., 2015; Ahuja *et al*., 2018). Cellulose is the main constituent of a plant cell wall, offering structural support and acting as a reinforcement element together with hemicellulose and lignin (Moran *et al.,* 2008; Galiwango *et al*., 2019). The last few decades have revealed the growing interest of industry and scientists on the research and development of polymeric materials from renewable sources (Poletto *et al*., 2014). Due to its non-toxic, renewable, biodegradable and readily modifiable properties, cellulose is attractive as a sustainable source of materials for industrial processes (Li *et al*., 2009). Therefore, extensive effort has been devoted to chemical and structural studies on cellulose (Bian *et al*., 2012).

Cellulose is a linear polysaccharide consisting of D-anhydroglucopyranose units (AGU), which are linked by β - (1 → 4) - glycosidic bonds (Lu *et al*., 2013). Anhydroglucose unit (AGU) is a single sugar molecule in a polymer and presented from three reactive hydroxyl groups: the primary OH on C(6) and the two secondary OHs on C(2) and C(3).These hydroxyl groups at C-2, C-3 and C-6 positions are capable of undergoing the typical reactions known for primary and secondary alcohols. The bridging and the ring oxygen atom are predominantly involved in intramolecular and intermolecular interactions, mainly hydrogen bonds and in degradation reactions (Klemm *et al*., 1998).

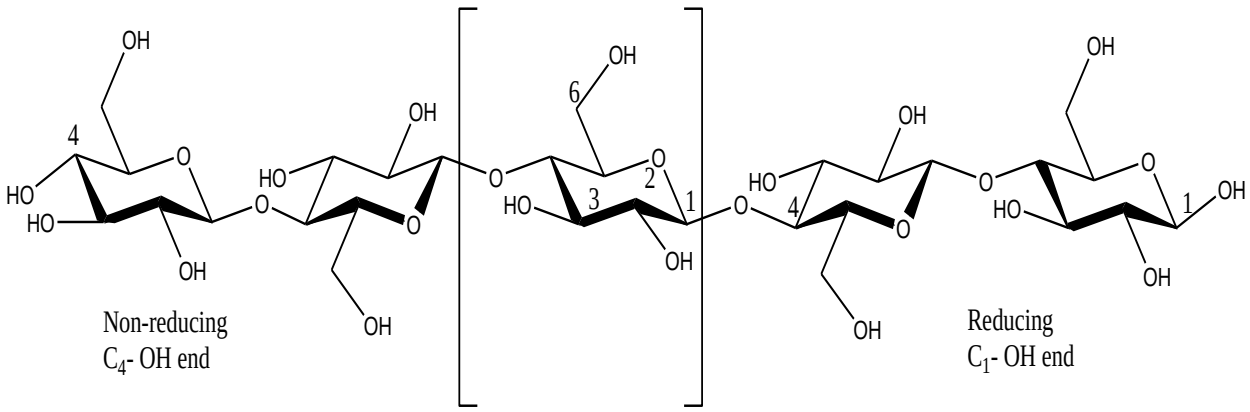

Figure 1: Molecular structure of cellulose with assignments of reaction sites in the AGU monomer: O-2, O-3 and O-6.

In the primary walls of growing plant cells, the glucose polymer cellulose is assembled into long microfibrils (Thomas *et al*., 2013). These microfibrils are surrounded by a non-cellulosic matrix of lignin and hemicellulose. Because of the presence of the three components, the sources of cellulose are usually known as lignocellulosic materials. In lignocellulosic material, cellulose is bonded together with hemicelluloses and lignin by covalent bonding, various intermolecular bridges, and van der Waals forces, forming a complex structure. Their structural composition varies with climatic and growth conditions, species, tissue and cell wall maturity of plants they are extracted from (Bian *et al*., 2012; Ahuja *et al*., 2018).

Hemicellulose is composed of different types of cycled saccharides such as xylose, mannose and glucose, among others. It forms a highly branched random structure. It is mainly amorphous (Moran *et al.,* 2008). Hemicellulose is a water-soluble polysaccharide (Abraham *et al*., 2011). Lignin is the second most abundant biopolymer after cellulose, the amorphous polymers formed by phenyl-propane units. It mainly consists of aromatic units such as guaiacyl, syringyl and phenylpropane (Ahuja *et al*., 2018; Moran *et al*., 2008). Lignin is a complex organic compound with alkali soluble character (Abraham *et al*., 2011).

Cellulose is generally known to be fibrillar, crystalline and exhibits its unique structural hierarchy of different biological origin. The cellulose fibrils play an important role in contributing to the high strength of plant cell walls (Lu *et al*., 2013). It is the main component of several natural fibers such as cotton, flax, hemp, jute and sisal (Moran *et al*., 2008). It is also distributed in some marine animals, fungi, bacteria, algae, invertebrates and even amoeba (Chen *et al*., 2016).

1.2. Industrial Sources of Cellulose

Wood and cotton are the major resources for all cellulose industrial products such as paper, textiles, construction materials, and cardboard, as well as for cellulose derivatives, such as cellulose esters (Biswas *et al*., 2006). Plant residue, particularly stems are lignocellulosic materials that could be considered as potential source for natural fibers (Vinayaka *et al*., 2017). The raw materials include, but are not restricted to, agricultural residues (sugarcane bagasse (Sun *et al*., 2004), Soy hulls (Neto *et al*., 2013) , wheat straw (Liu *et al*., 2005), rice straw (Fan *et al*., 2013), sweet sorghum bagasse (Kumar *et al*., 2015); woods (aspen (Jonasson *et al*., 2019), poplar (Chen *et al*., 2018), pine (Ditzel *et al*.,2017); waste newspaper (Rodrigues Filho *et al*., 2008); napier grass (Reddy *et al*., 2018) ; and industrial waste cotton

(Thambiraj and Shankaran, 2017; Chauhan *et al*., 2009), have been studied as sources of cellulose.

1.3. Cellulose from Cotton Linter

Cotton is one of the most important agricultural crops in many countries. It is one of the annual plants, primarily grown as textile raw material (Tutus, *et al*., 2017). The Ethiopia government gives special attention for the development of the textile sector which is one of the rapidly growing industries in Africa. Approximately 300 tons of dry cotton is produced each year in Ethiopia (Wagaye and Walle, 2018). Cotton linter (CL) is an unwanted part of finished fabrics that is not used in the textile process, which is considered as a waste material (Rahman *et al*., 2016). Huge mass of cellulosic wastes are produced as textile wastes in different garment and textile industries and that have virtually no use (Mondal and Alam, 2013). About 2.5 million metric tons of linters are produced annually throughout the world (Ibrahim and El-Zawawy, 2015).

CLs are short thick-walled, curly and cylindrical fibers that adhere to the cottonseeds after longer cotton fibers are extracted for textile use during a ginning process. The fuzzy seed needs to be subjected to an additional process that will mechanically remove the linter. They are removed by a mechanical delinting process for use in cellulose production by soda, sulfate, or organosolv pulping process (Bharimalla *et al*., 2017; Oun and Rhim, 2015).

Cotton linter is the most common sources of cellulose for industrial use. It has been used for making absorbent cotton and special papers (Ibrahim, 2002; Rahman, *et al*., 2016). When compared with wood, cellulose can be more easily obtained from linter. As an alternative to wood-based raw materials, linter cellulose is an important raw material resource for pulp and paper production. CL was first applied in regenerated cellulose production (Tutus, *et al*., 2017). In addition, CL is used in the production of cellulose esters such as nitro cellulose and cellulose acetate (Ibrahim and El-Zawawy, 2015).

Cotton linter (Figure 2) is a good raw material for preparation of cellulose due to its high degree of polymerization, crystallinity, purity and its higher content of cellulose (80% of holocellulose with 75% of alpha-cellulose) compared with other natural resources such as sisal (67–78%), bagasse of sugarcane (44.9–45%) and bamboo (41.8–54.0%) (Cheng, *et al*., 2017; Oun and Rhim, 2015).

Figure 2: Images of Cotton linter uncleaned (left) and cleaned (right) taken from Dukam ginning factory (Photo by M. Teshome).

Cotton linter is an agricultural residue/by-product that is generated by the garment processing industry. In Ethiopia, there are 21 ginning factories which produce large quantities of CL as a by-product every year. In addition, there are around 84 garment factories mostly located around Addis Ababa (Wagaye and Walle, 2018). Large volumes of textile waste are produced annually by those textile industries. Disposal of these solid wastes is becoming a major problem for the industry. As the rising cost, reduction in available space, and environmental issues are concerned, burning the textile waste and dumping to landfill sites are dwindling options (Dadi *et al*., 2017). The only added value of CL in Ethiopia is its use making pillow or bed mattress.

Therefore, collecting such huge quantity of by-product and find out the profitable application by producing valuable products such as cellulose and its cellulose derivatives such as cellulose acetate is quite attractive. This endeavour is also reduce the pollution related issue. In this study, cellulose acetate was produced from CL obtained from a ginning factory.

1.4. Cellulose Extraction Methods

Various methods have been suggested and used by different researchers to extract cellulose from different sources (Mzimela *et al*., 2018). Production of cellulose from lignocellulosic biomass requires pretreatment step. The delignification process allows removing impurities

such as wax, oils, pectin, lignin and hemicelluloses, leaving behind cellulose fibers (Husin *et al*., 2017; Tarchoun *et al*., 2019). In general, the pre-treatment methods can be classified into four different categories: physical, physio-chemical, chemical and biological processes. Physical pre-treatments (like milling, chipping and grinding) provoke an increase of the specific surface area. When performing physio-chemical processes like steam explosion or liquid hot water pretreatment, hemicellulose partially degrades and lignin can be depolymerised. The addition of acidic or alkaline solutions causes lignin to dissolve and hemicellulose to degrade (Rocha *et al*., 2012; Eisenhuber *et al*., 2013).

Chemical pretreatment methods are commonly used with the primary goal of removing lignin and/or hemicellulose (Ibrahim *et al*., 2013). Many studies have been made to isolate cellulose from various biomass sources, in which aqueous alkali extraction method followed by bleaching are the most commonly used methods for removing large amounts of hemicelluloses from the original or delignified lignocelluloses as well as pectin, waxes and hydrophobic or surface impurities (Bian *et al.*, 2012; Haleem *et al.*, 2014).

The alkali treatment involves the swelling of the crystalline region, and alkalisation of the peripheral hydroxyl groups that affect the molecular orientation of cellulose crystallites due to the removal of lignin and hemicellulose. It also increases surface roughness, resulting in a better mechanical interlocking and the amount of cellulose exposed on the fiber surface (Ibraham *et al*., 2013; Haleem *et al*., 2014). The alkali extraction treatment also allows the removal of soluble polysaccharides (Mzimela *et al*., 2018). Generally, alkali reagents remove the lignin component in the biomass mainly through the cleavage of α-ether linkages and ester bonds between lignin and hemicellulose molecules or by the hydrolysis of uronic and acetic esters (Dong *et al*., 2014).

Another chemical method of pretreatment is organosolvent methods of delignification. Organosolvent fractionation is a promising fractionation technology and comprises a class of processes in which lignocellulosic biomass is treated with a mix of an organic solvent and water, often at elevated temperatures. Commonly used solvents are ethanol, methanol, acetone and organic acids like acetic acid and formic acid or combinations thereof. Due to the process, cellulose is delignified, with the organic solvent functioning as lignin extraction solvent, and the hemicellulose is depolymerized through acid hydrolysis by the added acid or the acid that is formed from the acetyl side groups of the hemicellulose at elevated temperature (Snelders *et al*., 2014). In particular, as the main delignification reagent of the

cooking solution, peracetic acid is widely used, which is formed in the process of interaction of hydrogen peroxide and acetic acid (Barbash *et al*., 2017). In addition, acetic acid alone is also an efficient method to fractionate lignocellulosic materials (Pan and Sano, 2005).

Organosolv extraction by using formic acid is also recognized as an effective alternative method for delignification. As a cheap and readily available organic solvent, formic acid shows potential as a chemical agent for biomass fractionation. During formic acid pulping, lignin dissolves into black liquor due to cleavage of the lignin β-O-4 bonds, while hemicellulose degrades into mono- and oligosaccharides, leaving solid cellulose in the residue. When water is added to the liquor, lignin precipitates and separates from the liquor. Pulping of lignocellulose by formic acid is effective for delignification when formic acid concentration is higher than 80%, but delignification is inadequate at formic acid strengths below 70% (Zhang *et al*., 2010).

Biological pretreatment is another method used to isolate cellulose based on the use of microorganisms able to degrade lignin and hemicellulose. The method does not require a high amount of energy and can be carried out under normal conditions. Lignin and hemicellulose present in agricultural waste are degraded by microorganisms like brown and white-rot fungi as they possess lignin-degrading abilities. Enzymes such as peroxidases and laccases also facilitate lignin degradation (Arora *et al*., 2016). In addition, biological pretreatment, using bacteria (Actinomycetes) has been observed to be effective on grasses. However, biological pretreatment has a drawback that makes it less suitable for industry include a long residence time of 10–14 days, extremely precise growth conditions, and the need for a large space to perform the biological pretreatment. Another potential disadvantage is that some fraction of the carbohydrate is consumed by the microorganism (Amin *et al*., 2017).

Bleaching is another consecutive step in cellulose extraction. In bleaching technologies, there has been a growing interest in the use of hydrogen peroxide as one of the oxidants to replace chlorine-based reagents, because the by-products are environmentally benign (Sun *et al*., 2004). Although hydrogen peroxide treatment could remove less lignin than the alkali treatment, it plays an important role in improving fibers. Particularly, some functional structures in lignin macromolecules such as benzene ring in phenolic structure and side chain with carbonyl group or olefin aldehyde structure are not sensitive to alkali but can be destroyed by the oxidation of hydrogen peroxide. Therefore, the remained lignin components after alkali treatment could be further eliminated by hydrogen peroxide, which results in

looser internal structure and higher carding yield of the fibers (Dong *et al*., 2014). In general, bleaching process is required to achieve higher levels of whiteness and purity without loss of the physical and mechanical properties of the cellulose (Alves *et al*., 2019).

Because of the complexity of the cell wall structures, it is difficult to isolate pure cellulose from lignocellulosic material. Therefore, combined treatments, carried out as multi-stage or simultaneously, have shown to be more effective to fractionate lignocellulosic biomass than single treatments (Araujo *et al*., 2020). The combination of the chemical and mechanical treatments for lignocellulosic material involves the complete removal of matrix material (mainly hemicelluloses and lignin) to obtain relatively pure cellulose. Furthermore, they can also contribute to reducing costs, time of processing, as well as the use of chemicals and energy (Bian *et al*., 2012; Singh *et al*., 2020).

Steam explosion method

Several processes have been continuously developed to isolate cellulose from biomass, such as steam explosion, organosolv process chlorine-free method, combined chemical and enzymatic extraction (Fan *et al.*, 2013). Physical treatments, such as crushing and grinding, steam and irradiation, have been proven to be effective in creating accessibility to chemicals and enzymes (Chen *et al*., 2011). Among these methods, steam explosion is a green method with high efficiency to process biomass and could be performed on a large scale and become a well-known method for separating lignocellulosic material into its main components: cellulose, lignin, and hemicellulose (Dong *et al*., 2014; Ibrahim *et al*., 2010).

The steam explosion process was first introduced by Mason in 1927 to defibrillate wood fiber for board production. It is a high yield pulping process based on vapour phase at temperature in the range 80–210 $^{\circ}$C (Sonia and Dasan, 2013). During the steam explosion process, the raw material is exposed to pressurized steam, for short periods of time, followed by rapid reduction in pressure (sudden decompression) resulting in substantial break down of the lignocellulosic structure, hydrolysis of the hemicellulose fraction, depolymerization of the lignin components and defibrillization. The rapid release of pressure during steam explosion causes a loose structure of the natural fibers and increases the specific surface area (Cherian *et al*., 2010; Deepa *et al*., 2011; Yang *et al*., 2018). Effects of this process on biomass are: cleavage of some accessible glycosidic links, cleavage of β-ether linkages of lignin, cleavage

s of lignin–carbohydrate complex bonds and minor chemical modification of lignin and carbohydrates (Sonia and Dasan, 2013).

Steam explosion has been applied for the pretreatment of various lignocelluloses and also used to decrease the amount of alkali used during pretreatment. It is considered as an efficient method for the removal of hemicellulose and for the disruption of cellulose crystallinity. The steam treatment is an effective pretreatment process for fibers to destroy also lignin proportion (Ouyang *et al*., 2018; Punsuvon *et al*., 2008; Boonterm *et al*., 2015). During the steam explosion, significant amounts of hemicelluloses are partially hydrolysed and some lignin is depolymerised, giving rise to sugars and phenolic compounds that are soluble in water (Sun *et al*., 2005). Therefore, steam explosion facilitates subsequent chemical treatments and improves the removal efficiency of non-cellulosic materials because of the increased reactive surface it causes (Yang *et al*., 2018).

Alkaline peroxide post-treatment after pre-treatment with steam explosion, which is the method of interest in this study, resulted in substantial dissolution of lignin and an increase in cellulose crystallinity (Sun *et al*., 2005). Hydrogen peroxide is an effective agent for lignocellulose delignification. Alkaline can synergize hydrogen peroxide for lignocellulose pretreatment. Steam explosion, alkaline and hydrogen peroxide are effective methods for lignocellulose pretreatment, and their mechanisms of action are different. Therefore, the three treatment methods could synergize each other and the cellulose content can increase significantly after pretreatment of steam explosion coupling with alkaline peroxide (Chen *et al*., 2008).

Generally, to minimize the environmental impact due to chemical waste and maximize the extraction efficiency, the application of combined steam explosion and alkaline treatment are better with high cellulose yielding percentage (Boonterm *et al*., 2015). It can also facilitate the hydrolysis (i.e. degradation) of hemicellulose to glucose or xylose, resulting in the use of lesser amount of chemicals (Yang *et al*., 2017). In other words, steam explosion can make it easier to separate the cellulose from the lignocellulose materials in the further stages, making use of fewer chemicals, less time, and less money in terms of the overall processes (Phinichka and Kaenthong, 2018).

1.5. Cellulose Modification

Cellulose has limitations in its processability. It is neither meltable nor soluble in most common solvents because of the large amount of inter- and intramolecular hydrogen bonding and its high degree of cystallinity in structure. Therefore, the modification or conversion of cellulose to its derivatives renders it processible into various useful forms (Ratanakamnuan *et al*., 2012). Chemical modification of cellulose is one method of the production of value-added products (El Nemr *et al*., 2015). After chemical modifications, cellulose can provide several biodegradable cellulose derivatives, including carboxymethyl cellulose (CMC), hydroxypropylmethyl cellulose (HPMC) and cellulose acetate (CA). The production of cellulose derivatives has extensive interest worldwide, mainly because of its abundance in nature, its biodegradability and its lower environmental impact in comparison with polymers obtained from fossil sources (Nabili *et al*., 2017; El Nemr *et al*., 2017).

Among those various possible cellulose derivatives cellulose esters, specifically cellulose acetate (CA) or acetylation have been the most widely used and most successful chemical modification. It is an effective method to reduce the number of hydroxyl groups in cellulose, which accordingly increases hydrophobicity and diminishes hydrogen bonding. CA is one of the most industrial products with widely commercial applications (Gilbert and Palle, 2013; Zhou *et al*., 2016; El Nemr *et al*., 2015).

1.6. Cellulose Acetate

Cellulose acetate, as one of the most intensively studied cellulose derivative first synthesized by Schützenberger in 1865 by reacting cellulose with acetic anhydride heated in a closed tube at 180 °C. But it was not until 1904, when Miles found that partially saponified triacetate was soluble in acetone, that the commercial feasibility was recognized (Beraich *et al*., 2016; Barkalow *et al.,* 1989). However, in the early 1920s, cellulose acetate fiber was trial-produced successfully in UK and realized the industrialized production (Si *et al*., 2016).

Cellulose acetate, the by-product of cellulose modification is one of the most important esters of cellulose (Fischer *et al*., 2008). Cellulose which is composed β-1, 4-anhydro-D-glucopyranose units has high reactive hydroxyl groups that can be substituted by acetyl group to form cellulose acetate (Egot and Alguno, 2018).

Various methods have been developed for production of CA, in which acetic anhydride and acetyl chloride are commonly used as acetylating agents. Industrially, cellulose acetate is produced by cellulose acetylation, in which cellulose reacts in the presence of acetic anhydride that is used as acetylating agent, acetic acid used as a solvent, and sulfuric acid or perchloric acid used as catalyst (Djuned *et al*., 2014; Cerqueira *et al*., 2007). The acetylation process depends on the accessibility of cellulose fibers and the susceptibility of individual cellulose crystallites and the degree of substitution (DS) depend on experimental conditions (De Freitas *et al*., 2017; Barud *et al*., 2008). Another method for acetylation is the use of iodine as a catalyst for the esterification of cellulose in the presence of acetic anhydride (Cheng *et al*., 2010; Das *et al*., 2014). However, it is difficult to use iodine as a catalyst due to its solubility in most organic solvents and sublimation nature (El Nemr *et al*., 2017).

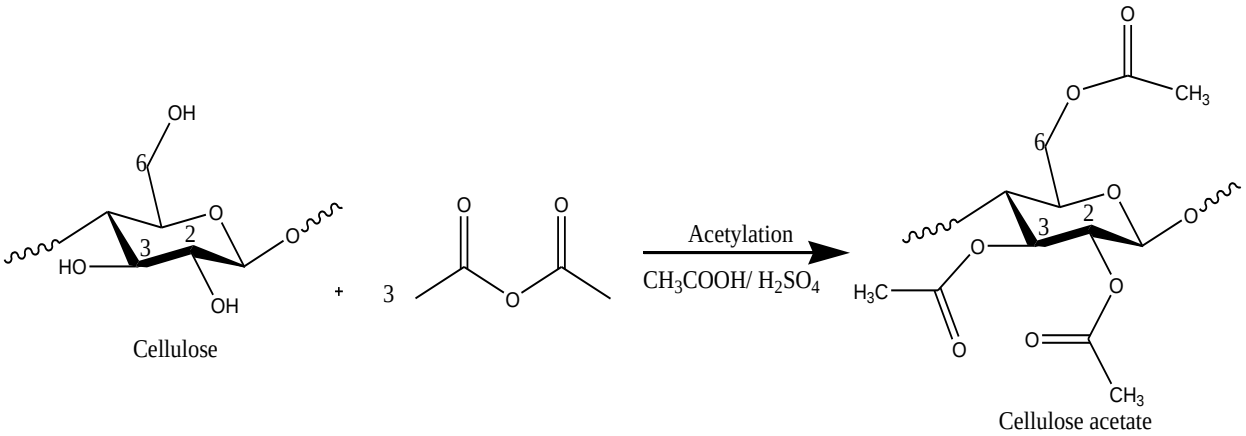

Figure 3: Scheme of acetylation of cellulose

The use of non-aqueous solvent system have been proposed as a reaction media for the derivatization of cellulose, allowing products to be made with a more homogeneous distribution of functional groups. Prominent among these systems are solutions N, N-dimethylacetamide (DMAc)/lithium chloride, ring-opening esterification and transesterification, which have been used to synthesize CA under heterogeneous or homogeneous condition (Ass *et al*., 2006). Transesterification is a relatively mild acetylation method, which uses acetate ester as an innocuous acyl donor, avoiding the formation and introduction of acidic reagents in the acetylation system (Cheng *et al*., 2010). Ionic liquids (ILs) have been also considered as efficient solvents for the acetylation of cellulose. However, long pretreatment and reaction times are usually required in these systems and their industrial application is limited due to cost issues (Chen *et al*., 2016).

1.7. Physico-chemical Characterization of Cellulose and Cellulose Acetate

Physico-chemical properties of natural fibers depend on the cellulose type because each type of cellulose has its own cell geometry and method used for isolation of cellulose. Physico-chemical properties of CA depend mainly on the DS. The physicochemical properties of cellulose and CA are summarized below.

1.7.1. Degree of polymerization

The chain length of cellulose is generally expressed as the degree of polymerization (DP), which is defined as the average number of anhydroglucose units in the chain of the cellulose molecules. The degree of polymerization (DP) of a cellulose sample varies between 100 and 15,000 and depends on the cellulose source as well as the method used for isolation. There are several methods for determining the DP of cellulose and CA, including the intrinsic viscosity methods in a suitable solvent (Galiwango *et al*., 2019; Ibrahim *et al*., 2010). Viscosity is a hydrodynamic property of polymer solutions which can be employed as an indicator of their DP (Bonet *et al*., 2005). The molecular weight of cellulose can be defined by its average DP (Ragab *et al*., 2014).

1.7.2. Degree of substitution and solubility

The physico-chemical properties of CA and their quality depend on the cellulose chain length, on the type, acetyl content and DS. Acetyl content of cellulose acetate is influenced by several factors such as cellulose with anhydride acetic ratio, acetylation time and interaction between treatment factors (Obeidat and Alzoubi, 2014; Bahmid *et al*., 2013).

The DS of cellulose acetate significantly influences material properties, particularly thermal properties, hydrophobicity, transparency, processability and solubility. The DS value is controlled effectively by adjusting the reaction time, temperature and molar ratio of derivatizing agent to cellulose (Cao *et al*., 2010). The DS of cellulose acetate can be determined by using different methods such as titration, FTIR and 1H-NMR.

Cellulose acetate solubility in organic solvents depends on the number of hydroxyl moieties substituted by acetyl groups (Gavila and Esposito, 2017). The solubility of CA also depends on the solubility parameter of the solvents in addition to the DS. Thus, CA with a DS between 0.5 and 1 are soluble in aqueous solutions, whereas those with DS 1 tend to be

insoluble in an aqueous medium, but soluble in organic solvents. In general, common solvents like tetrahydrofuran, methyl acetate, acetone and chloroform, can be used for DS higher than 2. This behaviour is quite distinct from natural cellulose, which cannot dissolve in common solvents and is difficult to process. As known, solvents contribute essentially to the modification of the solution behaviour (association, complex, micelle and core-shell structure of the polymer chains) and to processes establishing the membrane morphology of cellulose derivatives. Therefore, controlling DS of acetylated cellulose is clearly an important factor for practical applications (Ioan, *et al*., 2009; Zhou *et al*., 2016).

1.7.3. Crystallinity and polymorphism

In nature, the cellulose molecular chains are biosynthesized and self-assembled into microfibrils, which are composed of crystalline and amorphous domains (Lu *et al*., 2013). Crystalline region is more compact and neater compared with that of amorphous region (Kale *et al*., 2017). The crystalline cellulose is known to crystallize in several different polymorphs (Sun *et al*., 2005). Four different crystalline allomorphs of cellulose (cellulose I, II, III and IV), has been identified by their characteristic X-ray diffraction patterns and solid-state ^{13}C nuclear magnetic resonance (NMR) spectra (Mittal *et al*., 2011).

The most abundant native crystalline form is cellulose I (Abraham *et al*., 2011). It had long been believed that native cellulose was a unique structure. In 1984, however, Atalla and Vander Hart proposed that native celluloses consisted of two distinct crystalline allomorphs, namely cellulose Iα and Iβ (Wada *et al*., 2004). Cellulose Iα has one-chain triclinic structure and cellulose Iβ has two-chain monoclinic structure, and they differ in hydrogen bonding. Cellulose Iα is metastable and can be converted to the more stable form Iβ by heat (Sun *et al*., 2005). Cellulose Iα is the predominant form found in bacteria and algae, whereas the cellulose in higher plants is mostly Iβ (Mittal *et al*., 2011). Cellulose II can be prepared by two distinct routes, mercerization (alkali treatment) and regeneration (solubilization and subsequent recrystallization). Cellulose III and IV can be formed from cellulose I and II, respectively, by treatment with liquid ammonia; the reaction is, however, reversible (Abraham *et al*., 2011; Mittal *et al*., 2011).

Cellulose has an extremely high degree of crystallinity and this is due to the formation of several hydrogen bonds originating from its hydroxyl groups. Its high stereoregularity is also a contributory factor for its high crystallinity (Chauhan *et al.*, 2009). Crystallinity is an

important property that affects physical, mechanical, and chemical properties of cellulose. Tensile strength, dimensional stability, and density are known to increase with increasing cellulose crystallinity, while chemical reactivity and swelling decrease. The degree of crystallinity of cellulose varies from 60–80% depending on the source and chemo-mechanical treatment used (Agustin *et al*., 2015; Haafiz *et al*., 2013).

The physical properties of cellulose can be significantly modified by derivatization (Chen *et al*., 2016). In contrast to cellulose, CA possesses a much less crystalline structure. This reduction in crystallinity occurs due to the substitution of the hydroxyl groups by acetyl groups that have a greater volume (Barud *et al*., 2008). For instance, CAs with a low DS value have more crystalline structure and has potential for biodegradation as compared with CA with high DS, whereas a high DS value means more acetyl groups that disrupt the ordered structure of cellulose, leading to CAs with higher levels of acetylation and lower crystallinity, and also with increased swelling and solubility and improved storage stability (Fei *et al*., 2017). The degree of crystallinity of cellulose and CA can be determined by X-ray diffraction (XRD) (Haafiz *et al*., 2013).

1.7.4. Morphological characterization

The morphological structure of cellulose comprises a well-organized architecture of fibrillar elements. Cellulose is the smooth fiber surface that was shaped cylindrical fibers with the same size and had perforated layer (Bahmid *et al.,* 2013). The CA is irregular shaped fibrils, which are often aggregated and a rough surface morphology (El Nemr *et al*., 2017). Morphology of cellulose and CA can be studied by electron microscopy techniques such as scanning (SEM), transmission (TEM) electron microscopy and Atomic Force Microscopy (AFM) (Cao *et al*., 2016; Bhattacharya *et al*., 2008).

1.7.5. Thermal analysis

Fundamental information regarding the thermal stability of cellulose and CA can be obtained from thermogravimetric analysis (TGA) and DSC. TGA is commonly used to measure the change in weight of the material as a function of temperature in an inert atmosphere or in the presence of air or oxygen. Most polymers degrade if exposed to elevated temperatures, especially in air, and during manufacturing, when they are often exposed to thermal stress. Therefore, it is important to know the effects of the processing temperature associated with the processing duration (Deepa *et al*., 2011).

The thermal stability of cellulose fibers is affected by crystalline order, which decreases after substitution of cellulose hydroxyls with organic acids. Therefore, the thermal stability of cellulose esters is lower than that of original cellulose. However, the thermal properties of cellulose derivatives are sensitive to DS changes and to the uniformity of the substitution-group distribution. On the other hand, with increasing DS the decomposition temperature (Tdm) of cellulose esters increases. This improvement of thermal stability of cellulose esters may be explained by the formation of new-ordered structures in substituted regions (Jandura *et al*., 2000; Barud *et al*., 2008).

1.8. Application of Cellulose and Cellulose Acetate

A great deal of research efforts is being focused on cellulose due to its renewable nature, wide availability, low density, high specific strength and modulus, high aspect ratio, large reactive surface and wide applications in various industries. In paper industries it is used as a coating material on the surface of paper and paperboard thus improving the barrier properties, especially air resistance (Ahuja *et al*., 2018).

However, due to the intra and intermolecular interactions of the hydroxyl groups presented in the cellobiose unit, the cellulose molecules crystallize in a horizontal plane and in parallel chains, forming microfiber packages that limit its application (e.g., lack of antimicrobial properties, high hydrophilicity, low dimensional stability and high melting temperature) (Araujo *et al*., 2020). To overcome these drawbacks, cellulose is generally modified into derivatives. Due to their unique chemical and physical properties, derivatives of cellulose have been widely used in waste treatment, oil recovery, paper manufacturing, textile finishing, cosmetics, packaging and pharmaceutical application (Das *et al*., 2014; Ghareeb and Radke, 2013). Cellulose derivatives can also use in fabricating formulated foods for regulation of rheological properties, emulsification, stabilization of foams, modification of ice crystal formation, and long time water-binding (Hamad *et al*., 2016).

1.8.1. Pharmaceutical applications of the cellulose acetate

Among other uses, cellulose is widely employed as a raw material as an excipients. Cellulose derivatives have found several applications in the pharmaceutical industry as diluents, lubricants, disintegrants, binder, drug-release modifiers, suspending agents, mucoadhesive

agents, gelling agents and coatings in tablets and capsules manufacturing (Azubuike *et al*., 2011; Vora and Shah, 2015).

Of all cellulose derivatives, CA is a widely investigated and used both in the industry and in research for various applications, because of its excellent physical, chemical and biological properties. It has an excellent quality with good transparency, tensile strength, heat resistance, low water absorption, and biodegradable (Asman and Akçay, 2014; Bahmid *et al*., 2013). It is well known that the properties of CA, and hence its applications, depend on the DS which is the average value of acetyl groups replacing the hydroxyl groups in the anhydroglucose units (AGU) of cellulose (Fei *et al*., 2017). For example, cellulose diacetate (2-2.5) can be used for osmotic drug delivery and preparation of membranes for controlled drug release (Zhou *et al*., 2016).

Cellulose acetate is the water-insoluble cellulose derivatives and widely used in oral sustained release pharmaceutical formulations for production of matrices for controlled drug release, film-forming agent, microspheres and also used as coating material for semi-permeable membrane in controlled release drug delivery (Wan, *et al*., 2012; Brandao *et al*., 2013). It has many advantages for using in sustained release formulation, which include; water insolubility, making it insoluble throughout GIT, easily moulded and soluble in various organic solvents. It also used for taste masking and tableting (Kumar, *et al*., 2015; Asman and Akçay, 2014).

1.8.2. Other applications of the cellulose acetate

Depending on its processing, CA can be used for different applications such as films in photography, electrical insulators and cigarette filters (El Nmer *et al*., 2015; Zhou *et al*., 2016). It also used in manufacturing paint, packing material, laminates and artificial kidney (Cao *et al*., 2018).

1.9. Sustained Release Drug Delivery

Sustained release drug delivery systems are gaining popularity due to several reasons. It minimizes fluctuation in blood drug concentrations and reduces the frequency of dosing. It also provides a continuous mode of drug administration and enhanced patient compliance (Nadaf *et al*., 2015; Akpabio *et al*., 2016). Theophylline is an example of drug with a narrow

therapeutic range that may require drug monitoring both to achieve therapeutic levels and minimize toxicity. In order to overcome these problems, controlled release of theophylline seems to be the most appropriate preparation (Ojoe *et al*., 2007). Numerous efforts in drug development resulted in a number of controlled drug delivery systems consisting of a drug encapsulated within a suitable polymer carrier or equally dispersed in a polymeric matrix (Singh and Nath, 2012).

Sustained release matrix tablet can be prepared in two ways by using either hydrophilic polymer such as natural gums, HPMC, CMC, and hydrophobic polymer, like ethyl cellulose, cellulose acetate, eudragit and amylodextrin (Nadaf *et al*., 2015). One is direct compression of the powder blend containing the drug, polymer and other additives and another one involves granulation prior to compression. Selection of the proper method depends on the properties of the drug, polymer and other ingredients (Khan *et al*., 2019). Direct compression technology is scientifically and economically appealing since it entails reduced labour, cost, time, operational space, and equipment, and further no utilization of heat or moisture. In these directly compressed monolithic systems, the active agent is dispersed, dissolved or distributed in an inert polymeric diffusion barrier (Quadir *et al*., 2005; Reza *et al*., 2002)

1.10. Hydrophobic Matrix Tablets

Among various approaches for the preparation of controlled release tablets, matrix tablet is one of the least complicated approaches for obtaining controlled release and is widely used in industry. Because, it is simple, ease to manufacture, high level of reproducibility, stability of the raw materials and dosage form, and ease of scale-up (Vishwanadha *et al*., 2015; Nithya *et al*., 2014). Given the various options, polymers are versatile and promising agents to perform such functions (Rodrigo Filho *et al*., 2015). For any sustained release dosage form it is very important to use the minimum number of excipients with minimum processing steps in order to reduce the tablet-to-tablet and batch-to-batch variations, using direct compression technique as suitable (Ige *et al*., 2013). From different polymers, hydrophobic polymers are valuable in this regard because of their tablettability advantages over hydrophilic polymers (Obeidat and Alzoubi, 2014).

Hydrophobic polymers based matrix formulations have been used to control the release of drugs and can be produced using conventional processing equipment. It is widely used as a matrix in the preparation of both water soluble and sparingly water-soluble drugs. Its

inertness and its properties such as lack of toxicity, stability during storage and good compressibility make it suitable for designing sustained release matrices (Guerra-Ponce *et al*., 2016; Quadir *et al*., 2005). Cellulose acetate is also one of the components used in matrix systems for controlled release of drugs (Rodrigo Filho *et al*., 2015). However, the sustained release profile depends on physico-chemical properties of the drugs (Guyyonet *et al*., 1990).

1.11. Significance of the Study

A wide variety of plants has already been studied for the production of cellulose and its derivatives (Egot and Alguno, 2018). Among other cellulose sources, CL is being considered due to its abundance, availability, renewability, and low cost. It is the byproduct of textile industry, which contains valuable cellulose. Compared with wood and other agricultural waste, cotton linter has higher content of cellulose but lower hemicelluloses and lignin content (Cao *et al*., 2018; Liu, *et al*., 2011).

In Ethiopia, pharmaceutical industries import excipients by expending a large amount of foreign currency. However, the cost of drug development drives the quest to search for low-cost ingredients and enabling companies to enhance their existing products as well as to develop new drug delivery systems in order to cope with the global challenges and competition. Cellulose derivatives including CA are among the excipients frequently used in pharmaceutical industry for different purposes.

A lot of cotton linters are produced by cotton ginning factories in Ethiopia which are considered as waste materials and it has no value-added application in Ethiopia. The absence of a research report on cellulose and CA from CL in Ethiopia necessitates the need for preparation and characterization of CLC and CA from cotton linter.

Theophylline is chosen as a model drug for evaluation of CA prepared from CLC for sustained release tablet formulation. Theophylline is used as bronchodilators for moderate to severe reversible bronchospasm. It is also used in treating asthma and COPD. Its therapeutic serum concentration range is narrow from 5 - 15 µg/ml while toxicity usually appears at concentrations exceeding 20µg/ml. It's narrow therapeutic index which requires regular monitoring of serum theophylline concentrations. Therefore, sustained release forms of theophylline are used to avoid adverse effects and promote its more efficient use. In addition, it has a good thermal stability (melting between 270 and 274), and almost constant solubility

(1 g/120 ml) in a wide range of pH (pH 2 and 7.5), which are suitable properties for release tests (Rajalakshmi *et al*., 2011).

The present study therefore reports on the physico-chemical properties of the prepared CLC and CLCA in comparison with those of CCA and also with EC as potential sustained release excipient in theophylline tablet formulations.

1.12. Research Questions

1. What are the components of Cotton Linter?
2. What is the cellulose and CA yield of Cotton Linter?
3. What are the physico-chemical characteristics of CLC and CLCA?
4. How is the performance of CLCA powders as SR agents in tablet formulations?
5. What will be the mechanism of drug release the SR formulations prepared by CLCA?

1.13. Objectives

1.13.1. General objective

- To prepare and characterize CA prepared from CLC and evaluate its potential application as sustained release properties in theophylline tablet formulations.

1.13.2. Specific objectives

- To extract and characterize cellulose from cotton linter.
- To prepare and characterize CA from CLC.
- To evaluate the sustained release properties of CA from CLC in theophylline tablet formulations.
- To determine the drug release mechanism of SR tablets prepared by CLCA as a control releasing agent for SR tablet formulation.

2. EXPERIMENTAL

2.1. Raw Materials and Chemicals

Cotton linters (14 kg) were collected from Derry Kebede Cotton Ginning Factory PLC, Dukem, Ethiopia. Anhydrous theophylline (China Associate Co Ltd, China) was kindly donated by Addis Pharmaceuticals Factory PLC, Ethiopia. Acetic acid (99.9%) (Sigma Aldrich, Germany), Formic acid (85%), Ammonia solution (28%) (Farmitalia Carlo erba reagents S.P.A, Italy), Cupric sulphate pentahydrate (98.5%), Potassium iodide, Silica gel, Xylene (98%, extra pure), Zinc chloride (97%) (Loba Chemie Pvt. Ltd., India), Ethanol (96%) and Sodium chloride (99.8%) (UNI-CHEM, India), Hydrochloric acid (37%) (BDH Chemicals Ltd, England), Hydrogen peroxide (30%) (Carlo erba reagents S.A.S, France), Iodine (Hayashi pure chemical industries Ltd, Japan), Phenolphthalein, Magnesium stearate (Bulvinos Chemicals Ltd, England), Ethyl cellulose, Cellulose acetate, Sodium hydroxide (99.8%) (Alphax Chemical industry, India), and Toluene (99.5%) (Fisher Chemicals, UK), Acetic anhydride (May and Baker Ltd Dagenham, England), Chloroform, Acetone (99.5%), Sulphuric acid, Potassium dihydrogen phosphate (Sorensen, Leuren, Germany) were all used as received.

2.2. Methods

2.2.1. Determination of components of cotton linter

2.2.1.1. Solvent-extractable components

The components of CL were determined following the solvent extraction method (Mansor *et al*. 2019). In this, 60 mL of acetone were added to 1g CL (A) and placed in conical flask at 90 °C, over hot plate for 2 h. After 2 h, the sample was dried in an oven at 105 °C until constant weight was obtained (B). The extractive was determined from the Eq. 1.

Amount of extractive (g) =A - B……1

2.2.1.2. Hemicellulose

The amount of hemicellulose in CL was determined as follows:

First 150 mL of 0.5 M NaOH solution were added to 1 g of extractives free (B) CL and heated over a hot plate at 80 °C for 3.5 h. The sample was then washed with distilled water

and dried in an oven at 105 °C until a constant weight was obtained (C). The amount of hemicellulose was determined from Eq. 2.

Amount of hemicellulose (g) =B - C……2

2.2.1.3. Lignin

Thirty ml of 98 % sulphuric acid was added to 1 g of extractives free CL (B). The sample was then left at ambient temperature for 24 h; boiled at 100 °C on a hot plate for 1 h and the mixture was filtered and the solid residue was washed with distilled water. Finally, the sample was dried in an oven at 105 °C until a constant weight was obtained (D), which was recorded as lignin content.

2.2.2. Isolation of cellulose

During the preliminary work, isolation of cellulose from CL was carried out according to the following four methods: (i) Acetic acid-Nitric acid method, (ii) Peracetic acid method, (iii) Steam explosion and (iv) Formic acid-Acetic acid methods. In all these methods, extraction of cellulose from CL was carried out after dewaxing via mechanical pretreatment. Prior to any treatment, CL was washed with tap water and air dried. The dried CL was treated with toluene/ethanol (2:1, v/v) for 4 hrs at 60 ^{o}C with agitation with solid to liquor ratio of 1:50 w/v. After filtration, it was washed with ethanol repeatedly and dried in an oven (Kottermann® 2711, Germany) at 60 ^{o}C (Trache *et al*., 2014; Draman *et al.,* 2016; Singanusong *et al*., 2013; Fan *et al*., 2013).

In **acetic acid-nitric acid method**, 10 g of CL was treated with a 4% (w/w) NaOH solution containing 5 % (v/v) of hydrogen peroxide at 80 °C in water bath for 4 h at a liquid to solid ratio of 20:1. The solution was then filtered and washed repeatedly with distilled water. The CL-crude cellulose was then subjected to a rapid purification treatment with a mixture of 200 ml of 80% acetic acid and 20 ml of 68% nitric acid (v/v=10:1) at 100 °C for 15min. Finally, the residue was washed repeatedly with distilled water, filtered and dried at 60 ^{o}C to constant weight in an oven (Kottermann® 2711, Germany) (Liu *et al*., 2018).

In **peracetic acid method**, CL was treated with mixture of glacial acetic acid and 30% hydrogen peroxide in a volume ratio of 70:30 at the liquid to solid ratio 10:1, in water bath at 85^{o}C for 2 h. At the second stage, the alkaline treatment of CL was carried out with 8%

NaOH solution for 60 min at liquid to solid ratio of 12:1. Then, CL pulp was filtered and repeatedly washed with distilled water. Finally, the residue was dried at 60 ^{o}C to constant weight in an oven (Barbash, *et al*., 2017).

In the two-stage process based on **steam explosion** pre-treatment followed by alkaline peroxide post-treatment of the CL sample was carried out in an autoclave (Abraham *et al*., 2011; Sun *et al*., 2005). CL was steamed at 120 ^{o}C, 1.5 bar for 1 h with a solid to liquid ratio of 50:1. The residues (steam-exploded CL) recovered by filtration, were then thoroughly washed with distilled water. Then, residue from steam explosion was post-treated with 5% NaOH over a water bath at fiber liquor ratio of 1:20. The mixture was kept at 80 ^{o}C for 1 h. Finally, the mixture was treated with 10 % H_2O_2 and 1.6% NaOH at 65 ^{o}C for 2 h. The fibre to liquor ratio was 1:20. And, the residue was washed repeatedly with distilled water, filtered using nylon cloth and dried at 60 ^{o}C to constant weight in an oven.

In **formic acid-acetic acid** method, a mixture of 85% of formic acid and 99.5% acetic acid (at ratio of 50:30 by volume) at a fiber to liquor ratio of 1:8 were treated at 100 ^{o}C in hot plate for 2 h. Fibers were filtered and washed thoroughly with distilled water. The pulps were further treated with a mixture of Peroxyformic acid/Peroxyacetic acid (PFA/PAA) solution at 80 ^{o}C for 2 h at fiber to liquor ratio of 1:8. Peroxyformic acid /Peroxyacetic acid solution mixture was prepared in 2:2:1 ratio of 85% formic acid/ 99.5% Acetic acid/10%H_2O_2. Finally, the delignified fibers were bleached by treating at 1:10 pulp to liquor ratio with 8% H_2O_2 and 3% NaOH solution mixtures at 80 ^{o}C for 1 h. After filtration through nylon cloth, bleached fibers were washed with distilled water repeatedly and dried in an oven at 60 ^{o}C until constant weight was obtained (Jahan *et al*., 2014).

The cellulose characterized in the current study was isolated with steam explosion method followed by alkaline peroxide post-treatment. The CA powder characterized and evaluated for sustained release was also prepared following this extraction method.

2.2.3. Preparation of cellulose acetate

Acetylation of cellulose was carried out according to the method described by Shaikh *et al*. (2009). First, CLC (1.0 g) and acetic acid (18 mL) were placed in conical flask and the reaction mixture was stirred at room temperature for 1 h. Then, 5,6,7,8, to 9 ml of acetic anhydride were added in to CLC solution and the required amount of sulphuric acid was

added at different amount (0.05, 0.1, 0.2 and 0.3 ml). The mixture was heated to 25, 40, 55 and 70 ˚C and left for 30, 60, 90, 120 and 150 min with constant stirring using magnetic stirrer. The reaction mixture was slowly poured into 1L of distilled water with constant stirring for 1 h. Once the precipitation process was completed, the product was filtered and washed repeatedly with distilled water. Finally, it was dried in the oven at 60 °C until a constant weight was obtained.

2.2.4. Determination of percent yield

The yield of cellulose extracted from the CL and CLCA synthesized was measured on the dry weight basis. The cellulose yield, expressed as percentage, was calculated from Eq.3 and the CLCA yield was determined by dividing the dry weight of CLCA with weight of dried cellulose used as shown in Eq.4.

$$\text{Yield of cellulose (\%)} = \frac{\text{Weight of cellulose obtained (g)}}{\text{Weight of dried CL used(g)}} \text{x100\%} \quad \ldots\ldots\ldots\ldots\ldots\ldots\ldots 3$$

$$\text{Yield of CLCA (\%)} = \frac{\text{Weight of CA obtained (g)}}{\text{Weight of dried cellulose used(g)}} \text{ x100\%} \quad \ldots\ldots\ldots\ldots\ldots\ldots\ldots\ldots .. 4$$

2.2.5. Characterization of cellulose and cellulose acetate

2.2.5.1. Organoleptic characteristics

The colour, odour, taste and physical appearance of CLC and CLCA samples were observed.

2.2.5.2. Chemical identification test

Identification test of CLC was performed using iodinated zinc chloride solution. First, iodinated zinc chloride solution was prepared by dissolving 20 g of zinc chloride and 6.5 g of potassium iodide in 10.5 ml of distilled water. Then, 0.5 g of iodine was added and shaked for 15 min. About 10 mg of CLC was placed on a petri dish and dispersed in 2 ml of iodinated zinc chloride solution. The resulting colour of the substance was observed (USP 38/NF 33, 2015).

2.2.4.3. Determination of degree of polymerization

The DP of cellulose sample was determined according to the method described by Klemm *et al*. (1998) and Karande *et al.* (2011) by using cuprammonium hydroxide (Cuam) [Cu $(NH_3)_4(H2O)_2$] $(OH)_2$) solution as solvent. The Cuam solution was prepared by dissolving freshly precipitated Cu $(OH)_2$ in aqueous ammonia. Then, 100 mg of sample was added into 100 ml of Cuam solution. The mixture was vigorously shaken and then placed in a water bath at 25 ^{o}C for 5 min. After the sample was completely dissolved in the solvent, the viscosity of the solution was measured in an Ostwald Capillary viscometer (BDH, England). The viscosity was calculated from the efflux time of cellulose solution and the blank Cuam solution (Eq. 5).

$$\eta spec = \frac{\eta}{\eta 0} - 1 \quad \text{.....5}$$

Where, ηspec is specific viscosity; $\frac{\eta}{\eta 0}$ is relative viscosity η0 is the time required for the solvent to travel from upper graduated mark to the lower graduated mark and η is the time required for the sample to travel from upper graduated mark to the lower graduated mark.

The obtained ηspec was then used to calculate the DP of CLC based on eqn 6.

$$\text{DP of cellulose} = \frac{2000 \text{x } \eta spec}{c \text{ x } (1 + 0.29 \text{ x } \eta spec)} \quad \text{.....6}$$

Where, c is concentration (in g/L) of cellulose and 0.29 is viscometer constant.

The molecular weight of cellulose sample was determined from DP by using Eq.7.

M. Wt of cellulose = DP x 162.....7

The determination was performed in triplicate

On the other hand, the DP of the CLCA was determined according to international standard test methods of testing cellulose acetate (ASTM D 871-96 (2010). Initially, 0.26 g of sample was dried at temperature of 105 $^{\circ}$C for 2 h. Then, the sample was weighed and transferred to a 250-mL conical flask. The 100 ml of solvent were prepared from acetone (90%) and ethyl alcohol (10%) and poured into the flask containing the sample at 25 $^{\circ}$C. The mixture was then vigorously shaken and then placed in a water bath at 25 ^{o}C until the sample was completely dissolved. The viscosity of the solution was then measured in an Ostwald Capillary viscometer (BDH, England).

The viscosity was calculated from the efflux time of cellulose acetate solution and of the blank solution as per the following relationships (Eqs.8 and 9).

Relative viscosity, [ηre] $= \frac{\eta}{\eta 0}$ ……8

Intrinsic viscosity, [η]= $\left(\frac{10}{C}\right)[a\text{ntilog}\left(\frac{log\eta re}{10}\right) - 1]$……..9

From the intrinsic viscosity, the degree of polymerization (DP) of CA was calculated using Eq. 10.

DP $= 147x[\eta]^{1.2}$……..10

Finally, the molecular weight of cellulose acetate sample was calculated based on Eq.11.

Molecular weight (M_w) =DP x (159+ (DSx43) + (3-DS))……11

The determinations were performed in triplicate

2.2.4.4. Determination of acetyl group and degree of substitution of cellulose acetate

Acetyl group and DS of the CLCA were determined by titrimetric method. Accordingly, 0.1 g of cellulose acetate was added to 5 mL of 0.25 molL^{-1}NaOH and 5 mL of 75% ethanol. The mixture was left to stand for 24 h. After that, 10 MolL^{-1} of 0.25 M HCl was added to the mixture and the system was left to stand for 30 min. Subsequently, the mixture was titrated by a standard 0.25 molL^{-1} NaOH solution, using phenolphthalein as indicator. The same procedure was also done for a control system (without CA). This procedure was carried out in triplicate (Candido *et al*., 2016).

The percentage of acetyl groups (%AG) was calculated from the following equation

%Acetyl= $\frac{\{[(\text{VNaOH x A}) - (\text{VHclxB})]\ [(\text{V}'\text{NaOH x A}) - (\text{V}'\text{HCl xB})]\}\text{x } 43}{\text{w}}$……12

The % AG value then used to calculate the DS as per Eq.13.

DS= $\frac{162\text{x (\%Acetyl)}}{(4305 - 43\text{x\%Acetyl})}$…… 13

Where: % Acetyl is the percentage of acetyl groups in the sample; A is the concentration of NaOH solution in mol/L; B is the concentration of HCl solution in mol/L; VNaOH and V'NaOH are the volumes (L) of the NaOH solution added in the samples and in blank, respectively; VHCl and V'HCl are the volumes (L) of HCl added in the samples and in the

blank and W is the mass of the CA sample used,162 = molar weight of cellulose monomer and 43 = molar weight of acetyl group

2.2.4.5. Determination of free acid

The free acid in the CLCA and CCA sample were determined using titrimetric system. First, 5 g of CLCA and CCA were transferred into a 250-mL flask and 150 mL of distilled water was added. Then, the flask was closed with stopper gently swirled and allowed to stand for 3 h. The sample was filtered through whatman filter paper and the flask was washed with distilled water and washing was added to the filtrate. Then, phenolphthalein was added to the combined filtrate and washings and titrated with the 0.01N sodium hydroxide (USP38/NF33, 2015).

The percentage of free acid was calculated using equation 14.

$$\% \text{ Free acid} = \left(\frac{v}{w}\right) x 0.06005 \quad \ldots\ldots\ldots\ldots\ldots\ldots\ldots\ldots\ldots\ldots\ldots\ldots\ldots\ldots\ldots\ldots\ldots\ldots\ldots\ldots\ldots\ldots 14$$

Where, V is the volume of titrant consumed (mL) and W is the weight of CA used.

2.2.4.6. Determination of moisture content

The moisture content was determined according to the USP38/NF33, (2015). A 3 g of each CLC, CLCA and CCA sample were placed on pre-weighed Petri dish and weighed. Then the Petri dish was placed in an oven (Kottermann® 2711, Germany) and heated at 105 °C for 3 h. The samples were then taken out of an oven and weighed. The samples were then replaced in an oven for 30 min and reweighed. This procedure was continued until a mass loss of not more than 5 mg for 30 min drying time. The results were expressed as a mean of three parallel determinations and the percentage of moisture was calculated from Eq.15.

$$\text{Moisture } \% = \frac{\text{Gram loss on heating}}{\text{Gram of sample used}} \text{ x100} \quad \ldots\ldots\ldots\ldots\ldots\ldots\ldots\ldots\ldots\ldots\ldots\ldots\ldots\ldots\ldots\ldots\ldots\ldots\ldots\ldots\ldots\ldots 15$$

2.2.4.7. pH determination

Two of each g CLC, CLCA and CA were shaken manually with 100 ml of distilled water for 5 min, and allowed to stand. Then, the pH of the supernatant was determined by using pH meter (JENWAY, 3505, UK). All results are the mean of three parallel determinations.

2.2.4.8. Solubility test

The solubility test of CA was determined as per as the method described by Beraich *et al*. (2016). Accordingly, 1 g of CA was dissolved in 100 ml of distilled water, acetone and chloroform for about 30 min at ambient temperature with a continuous stirring using magnetic stirrer.

2.2.4.9. Ash value

The ash value of CLCA was determined according to the following procedure. A crucible was cleaned and oven dried at 100 ^{o}C for 30 min. Following cooling for 30 min in a desiccator which contains silica gel, the crucible weight was determined. Then, 3 g of CLCA samples were placed on the crucible and heated till smoking was stopped. The residue was then charred in a furnace at 550 °C for 2 h. After cooling in desiccator for 45–60 min, the weight of ash was determined and the ash value was calculated as weight percentage of the ratio of charred residue and the CA sample used.

2.2.4.10. Fourier transform infrared spectroscopy (FTIR)

Fourier transform infrared (FTIR) spectra of CLC, CLCA and CCA samples were acquired at room temperature using FTIR spectrophotometer (FTIR-8400S, SHIMADZU, Japan) in transmittance mode. Initially, the KBr disc was rinsed with alcohol. Then, about 5 to 10 mg finely ground samples were dissolved in liquid paraffin using a mortar and pestle and coated with KBr. The KBr along with the sample was placed in KBr holder and eventually inserted into the FTIR machine. Each IR spectrum was collected with 20 scans. Scanning was performed between wave numbers 4,000 and 400 cm^{-1}. The background spectrum was collected before running each sample.

2.2.4.11. X-ray diffraction (XRD)

To determine the crystal structure and crystallinity, XRD patterns of CLC, CLCA and CCA samples were first dried in a dry oven at 100 °C for 30 min and then measured with automated powder X-ray diffractometer (XRD-7000S SHIMADZU, Japan). In this, the samples were placed in the cavity of a disc sample holder of the diffractometer. The XRD data were generated with Cu-Ka radiation (λ = 1.542° A) at 40 kV voltage and 30 mA current

2θ angle range of 10°–40°, angle step of 0.02°, a time step of 0.4 seconds and scan speed of 3°/minute.

The crystalline indexes (CrI) of the samples were calculated from the X-ray diffraction patterns based on the peak height method developed by Segal *et al*. (1959) as shown in Eq.16

$$\text{CrI}\ (\%) = \frac{(\text{I002} - \text{Iam})}{I002} \text{ x100} \quad \text{.....16}$$

Where, I_{002} represents crystalline material and I_{am} represents the amorphous material.

2.2.4.12. Morphological characterization

The morphologies of CLC and CLCA DS 2.46 were studied using scanning electron microscopes (Carl Zeiss MA15 / EVO 18 scanning electron microscope, Germany). The scanning electron micrographs were taken at an accelerating voltage of 30 KV. The samples were then viewed and photomicrographs of the samples were taken.

2.2.4.13. Thermal analysis

The thermal properties of CLC, CLCA and CCA were determined with a thermogravimetric analyser (TA- Instruments SDT Q600, Japan). Initial weight of CLC, CLCA DS 0.83, CLCA DS 2.46 and CCA samples of 8.844, 23.603,30.489 and 16.156 mg, respectively, were subjected to TGA in a nitrogen atmosphere (100 ml/min), at a heating rate of 10°C/min and a temperature range of 22°C-700 $^{\circ}$C (Candido *et al*., 2016). Weight loss was recorded as a function of time and temperature.

2.2.6. Characterization of powder properties of cellulose acetate

2.2.6.1. Densities and related properties

Bulk density

For the measurement of bulk densities of CLCA, CCA and EC powders, 30 g of each of the powder were introduced into a 250 ml measuring cylinder. The cylinder was then lightly tapped twice to collect all the powder sticking on the wall of the cylinder. The volume was then read directly from the cylinder and used to calculate the bulk density. The average value of three independent determinations was finally taken. Bulk density (ρb) was determined from Eq. 17.

$$\rho b = \frac{m}{Vb} \quad \text{.....17}$$

Where, m is the weight of the powder and Vb is bulk volume.

Tapped density

A sample in measuring cylinder was placed on a tapped densitometer (ERWEKA, Germany). And samples were tapped sequentially 10, 500 and 1,250 times. Tapping was stopped when the change in volume didn't exceed 2 mL. The tapped density was calculated from the weight and tapped volume (V_t) of the powder. Tapped density (ρt) was determined as a mean of three measurements from Eq. 18 (USP38/NF33, 2015).

$$\rho t = \frac{m}{Vt} \quad \text{.....18}$$

Where, m is the weight of the powder and V_t is the tapped volume.

Hausner ratio and Carr's index

Hausner ratio and Carr's index (% compressibility) were calculated from the data of bulk and tapped density from Eq. 19 and 20, respectively.

$$\text{Hausner's ratio} = \frac{\rho t}{\rho b} \quad \text{..... 19}$$

$$\text{Carr's index (\%)} = \frac{\rho t - \rho b}{\rho t} \text{ X } 100 \quad \text{..... 20}$$

Where, ρt is the tapped density and ρb is the bulk density.

True density

True density was determined by liquid displacement method using xylene as an immersion fluid as follow. The CA sample was placed in a pycnometer; closed and weighed. Sufficient xylene was added to wash down and overlay the sample. After 10 min, the sediment CA was stirred with a small glass-stirring rod to release entrapped air. When the evolution of minute air bubbles through the supernatant xylene layer had stopped, the stirrer was removed and rinsed into the pycnometer with several ml of xylene. The sample was then allowed to settle and the volume was adjusted with xylene to 25 mL. True density (g/ml) was calculated from Eq. 21.

True density was measured as a mean of three measurements.

$$\rho = \frac{(W1 \times SG)}{[(W1 + W2) - W3]} \quad \text{.....21}$$

Where, ρ = true density of CA, W1= weight (g) of CA, W2= weight (g) of the pycnometer filled with xylene, W3= weight (g) of pycnometer with CA plus xylene, and SG = specific gravity of xylene (g/ml) (~0.862).

Flow rate and angle of repose

Flow rate and angle of repose were determined by fixed funnel- method. 13 g of CA powder were placed and allowed to flow through a stemless funnel having 10 mm aperture from a fixed height of 10 cm. The duration of flow was recorded and used to calculate the flow rate. The diameter of the powder cone and height was measured and angle of repose was calculated using equation 22.

$$\theta = tan^{-1}\left(\frac{h}{r}\right) \quad \text{..... 22}$$

Where, θ=Angle of repose, h = Height of powder and r = Radius of circle formed by the powder.

2.2.6.2. Moisture sorption pattern

Moisture sorption capacity was determined using the method described by Beever and Valentine (1958) and Mihranyan *et al*. (2004). Prior to moisture sorption determination, the CA sample was dried in oven at 105 ^{o}C for 4 h. Dried sample of 1g was spread evenly on plastic plate (pre-weighed) and placed in desiccators containing distilled water (100% RH), saturated solution of NaCl (75.6%) and appropriate concentrations of NaOH at 24.66%, 31.58% and 40% of NaOH solutions to provide 60%, 40% and 20% RH, respectively and stored at room temperature. Samples were equilibrated for four weeks and then the moisture uptake of each sample was calculated as the weight difference before and after equilibration in a given RH. Water sorption capacities of the CLCA and CCA were expressed as percent moisture sorbed.

2.2.6.3. Kawakita analysis

Compressibility and cohesiveness were determined following the Kawakita analysis (Pati *et al*. 2016). Accordingly, 30 g of sample powders were poured into a 250 mL glass measuring cylinder. The heaped particles in the cylinder were then leveled off horizontally with a thin metallic spatula and the bulk volume Vo was measured. Tapping was afterwards initiated mechanically and the change in volume of the powder column Vn was noted after *N* number of taps. The Kawakita equation is given by:

$$N/C = \frac{N}{a} + \frac{1}{ab} \quad \text{.....23}$$

Where a and b are constants; a describes the degree of volume reduction 1/b is considered to be a constant related to cohesion and C being the degree of volume reduction is calculated from the initial volume Vo and tapped volume Vn as:

$$C = \frac{(Vo - Vn)}{V0} \quad \text{.....24}$$

From the graphical presentation of N/C versus N (N = 5, 10, 20, 30, 40, 50, 75, 100, 300, 400 and 500), the constants were evaluated.

2.2.7. Drug-excipient interaction study

Drug-excipient interaction was investigated by FTIR spectroscopy as described in Section 2.2.4.10. The FTIR spectra of anhydrous theophylline powder alone and its physical mixture with CA sample (1:1) at 4000 cm^{-1} – 45 cm^{-1} were recorded using FTIR-8400S, Shimadzu, Japan.

2.2.8. Tablet preparation and evaluation

2.2.8.1. Tablet preparation

Matrix tablets of 400 mg were prepared by direct compression method with composition shown in Table. CLCA, CCA and EC powders were dry mixed with anhydrous theophylline in a Turbula mixer (Willy A. Bachofen AG, Turbula 2TF, Basel, Switzerland) for 5 min. Then, the mixtures were lubricated with 0.5% magnesium stearate for 3 min. Tablets were compressed in a rotary tablet compression machine (ECO PRESS 200, India) fitted with 11 mm punches at a fixed compression pressure. Similarly, plain tablets of CLCA, CCA and EC were also compressed using the same condition.

Table 1: The compositions of tablet formulations used in drug release studies.

Ingredients	**Formulations**					
	F1	F2	F3	F4	F5	F6
Theophylline (w/w %)	20	30	40	20	20	20
CLCA DS 2.46 (w/w %)	79.5	69.5	59.5	-	-	-
CLCA DS 0.83 (w/w %)	-	-	-	79.5	-	-
CCA (w/w %)	-	-	-	-	79.5	-
EC (w/w %)	-	-	-	-	-	79.5
Mg. stearate (w/w %)	0.5	0.5	0.5	0.5	0.5	0.5

Key - CLCA: cotton linter cellulose acetate, DS: degree of substitution, CCA: commercial cellulose acetate, EC: ethyl cellulose.

2.2.8.2. Tablet evaluation

2.2.8.2.1. Weight and thickness

From each batch, 20 tablets were randomly selected and weighed individually on an analytical balance (Mettler Toledo, PR 203, Switzerland) and then the average weight and standard deviation were calculated. Ten tablets were taken randomly from each batch and the thickness of each tablet was measured with a sliding caliper scale (Nippon Sokutei, Japan).

2.2.8.2.2. Crushing strength

Crushing strength of the tablets was determined using crushing strength tester (Caleva, THT2, England). Ten tablets were taken randomly from each batch and the crushing strengths of the tablets were measured individually, the means and standard deviations were calculated.

2.2.8.2.3. Tensile strength

The radial tensile strengths (σ) of the tablets were determined form Eq. 25.

$$\sigma = \frac{2xF}{\pi \text{ x } T \text{ x } D} \quad \text{.....25}$$

Where, F is the force required to break the tablets; D and T are the diameter and thickness of the tablets, respectively.

2.2.8.2.4. Friability

The friability of the tablets was determined using a friability tester (ERWEKA, TAR 20, Germany). Ten tablets of known weight were placed into friability tester and subjected rotation at speed of 25 rpm for 4 min. The tablet samples were then removed, dedusted and reweighed. Loss of tablet weight with respect to the initial value was then calculated as percent friability.

2.2.8.2.5. Porosity

Porosity (ε) of tablets was calculated according to Eq. 26.

$$\varepsilon = \left[1 - \frac{m/v}{\rho m}\right] \times 100 \quad \ldots \ldots \ldots 26$$

Where, m is the weight of the tablets, V is the volume of the tablets that is $V=\pi r^2 h$, where r is the radius, and h is the thickness of the compact, and ρm is the true density of materials.

2.2.8.2.6. Disintegration test

The disintegration test was carried out according to USP 38/NF 33 specifications (2015). Six tablets of known weight from each batch were placed in a disintegration tester (ERWEKA, DT504, Germany) filled with distilled water and maintained at temperature of 37 ± 2 ^{o}C. The tablets were considered completely disintegrated when all the particles passed through the wire mesh. The average disintegration time of six tablets was determined.

2.2.8.2.7. Construction of calibration curve

Aliquots of stock solution (50µg/ml) of anhydrous theophylline in 0.1 N HCl and phosphate buffer solution pH 6.8 were pipetted into a series of 100 ml volumetric flask and diluted to volume to provide different concentrations in the range of 4 µg/ml to 13µg/ml. Then, the absorbance of each of these serial dilutions was measured at the λmax (271 nm) by using UV-Visible spectrophotometer (T92+, UK). A 0.1 N HCl and phosphate buffer pH 6.8 were used as blank sample. The absorbance versus concentration of the solutions was plotted, and a linear regression equation and correlation coefficient were obtained.

2.2.8.2.8. *In vitro* drug dissolution

The *in vitro* drug release studies were performed according to USP/NF specification (USP38/NF33, 2015) in USP Dissolution Apparatus I (ERWEKA. DT600. Germany). The basket was adjusted to rotate at 100 rpm. A dissolution medium (900 ml) of 0.1 N HCL for the first 2 h and phosphate buffer solution of pH 6.8 for remaining 10 h, maintained at 37 ± 0.5 $^{\circ}$C, were used. Samples of 5 ml dissolution medium were withdrawn at predetermined time intervals of 0.25, 0.5 1, 2, 3, 4, 6, 8, 10 and 12 h. Each withdrawn sample was immediately replaced with an equal volume of the dissolution medium. The withdrawn samples were filtered, suitably diluted and UV absorbance readings were taken at 271 nm using UV spectrophotometer. Concentration of drug was determined from the standard calibration curve of theophylline and finally the results were plotted as cumulative % drug release versus time.

2.2.8.2.9. Analysis of drug release kinetics

The *in vitro* release data were fitted into the various drug release models (Eq.27-31) to evaluate the drug release kinetics from the matrix tablets:

I. Zero order release model: $Q = Qo - Kt$ … … … … … … … … … … … … …… 27

Where, Q is the amount of drug remaining at time t, Qo is the quantity of drug present initially in the dosage form and K is the zero-order release constant.

II. First order release model: $lnQ = \ln Qo - Kt$ … … … … … … … … …. … … … 28

Where, Q is the amount of drug remaining at time t, Qo is the quantity of drug present initially in the dosage form and K is the first order release constant.

III. Higuchi square root model: $Mt/Mo = Kt^{1/2}$ … … … … … … … … … … … … … 29

Where, Mt is the amount of drug released at time t, Mo the amount of total drug in tablets, Mt/Mo is the fractional drug release at time t and K is a constant incorporating the matrix structure.

IV. Korsmeyer-Peppas release model: $Mt/Mo = Kt^{n}$ … … … … … … … … … … …30

Where, Mt is the amount of drug released at time t, Mo the amount of total drug in tablets, Mt/Mo is the fractional drug release at time t, K is a constant incorporating the matrix structure and n is a diffusional exponent.

V. Hixson-Crowell cube root model: $Qo^{1/3} - Qt^{1/3} = Kt$ … … … … … … … … … … ……31

Where, Qt is the amount of drug remaining in time t, Qo is the initial amount of the drug in tablet and K is the rate constant for Hixson-Crowell rate equation.

The following plots were constructed using the *in-vitro* drug release data:

A. Cumulative % drug release versus time (Zero order release model);
B. Ln cumulative of % drug released versus time (First order release model);
C. Cumulative % drug release versus square root of time (Higuchi square root model);
D. Log cumulative % drug release versus log time (Korsmeyer-Peppas release model) and
E. Cube root of drug % remaining in matrix versus time (Hixson-Crowell cube root model).

2.2.9. Statistical analysis

Statistical analysis was carried out using Analysis of Variance (ANOVA) with statistical software Origin 8.5 (Origin Lab TM Corporation, USA). Each study was conducted in triplicate, and results are reported as mean ±standard deviation.

3. RESULTS AND DISCUSSION

3.1. Physico-chemical Properties of Cellulose and Cellulose Acetate

3.1.1. Components of cotton linter

The chemical compositions of untreated CL are shown in Table 2. The value of total extract of present study was lower than study reported by Morais *et al*. (2013) from CL (5.59 ± 1.9%). However, the value for lignin and hemicellulose were slightly higher as compared to value of 5.9±0.0%, 3.6 ± 0.6%, respectively reported by Bezzera *et al*. (2016) from CL. This difference may be due to environmental factors, method used for extraction and type of CL used.

Table 2: Components of cotton linter

Components	**Values (%)**
Total extract	3.12±0.34
Lignin	9.83±0.76
Hemicellulose	4.51± 0.27

3.1.2. Organoleptic characteristics and chemical identification test

The organoleptic properties of the prepared cellulose and CA samples fulfilled USP/NF specifications (Table 3). Organoleptically, the CLC obtained was white and fibrous nature (Figure 4a). The CLCAs were white, odourless and tasteless. The CLCA with DS 0.83 physically appeared as fine powder while CLCA DS 2.46 was granular powder as illustrated in Figure 4b. The identification test on CLC and sample cellulose with iodinated zinc chloride solution turned to violet-blue colour confirming the presence of CLC in the sample.

Table 3: Organoleptic Characteristics of CLC and CLCA

Organoleptic characteristics	**CLC**	**CLCA DS 0.83**	**CLCA DS 2.46**
Colour	White	White	White
Odour	Odourless	Odourless	Odourless
Taste	Tasteless	Tasteless	Tasteless
Physical appearance	Fibrous	Fine powder	Granular powder

Key- CLC: Cotton linter cellulose, CLCA: Cotton linter cellulose acetate, DS: degree of substitution

3.1.3. Percent yield of cellulose

The cellulose yield primarily depends on the method of extraction. The different extraction methods used during preliminary study resulted in different yields and qualities of cellulose fibers (Figure 4). The percentage yield of cellulose was 73.57%±1.25 (in acetic acid-nitric acid method), 80.64% ± 1.56 (peracetic acid method), 78.06%±1.70 (steam-alkali method) and 76.43%± 2.01(formic-acetic acid method).

From those methods, steam and formic-acetic methods gave white fiber, however the formic-acetic acid method provided lower yield by about 1.63% as compared with steam-alkali method. The differences in yield may be due to higher degradation of cellulose in those pretreatments. The peracetic method gave higher yield than the other methods but the obtained fiber was off white as shown in Figure 4a. Due to the fact that the obtained yield was reasonably high and small amount of chemicals are required for extraction, the steam-alkali based method of extraction was selected for extraction and characterization of CLC, CLCA thereof and evaluates CLCA as sustained release excipient in theophylline tablet formulation.

a)

b)

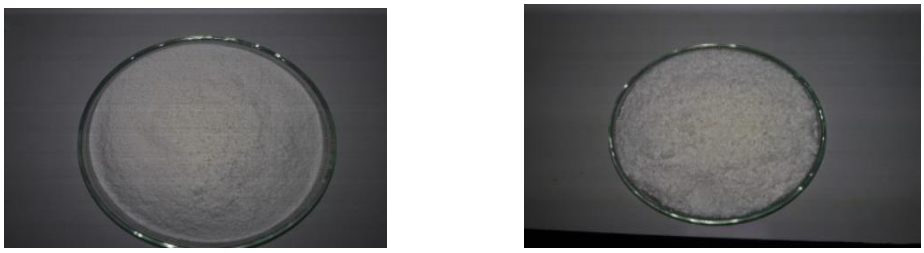

CLCA DS 0.83 CLCA DS 2.46

Figure 4: Cellulose (top) isolated from cotton linter following acetic-nitric acid, peracetic acid, steam-alkali and formic-acetic acid (left to right) treatment and cellulose acetate prepared from steam-alkali treated cellulose (bottom).

The cellulose yield obtained from steam-alkali extraction method (steam followed by alkali peroxide) was comparable with a previously reported study cellulose yield isolated from cotton gin waste (78.37%) and from cotton linter (80.88%) (Ibrahim *et al*., 2010; Gumuskaya *et al*., 2003). The slightly lower yield of cellulose in the present study might be associated with the method used for isolation of cellulose and type of cotton linter used. However, the yield of this study was higher than the yield of cellulose isolated from sorghum straw (47.38%) and sugarcane bagasse (44.7%) (Alves *et al*., 2019; Sun *et al*., 2004). Obviously, these differences are mainly due to the type of samples used for cellulose isolation.

3.1.4. Degree of substitution and yield of cellulose acetate

The influence of the concentration of acetic anhydride, sulphuric acid as a catalyst, the reaction time and temperature on the yield and DS of the CLCA due to acetylation are given in Table 4. Acetylation carried out at temperature ranging from 25 - 70 ◦C and reaction time ranging from 30 - 150 minutes provided CLCA powders with DS values ranging from 0.74 to 2.46.

The % yield of CLCA increased as the reaction time and temperature were increased. At the optimum temperature 55 ◦C the maximum % yield was obtained. The % yield of CLCA started to fall down with temperature above 55 ◦C and increasing reaction time (150 min). The DS value also displayed similar trend as shown in Table 4. The reason for this enhancement of the acetylation reaction with increasing temperature and reaction time was probably because high temperatures can cause swelling of cellulose and also increase the diffusion rate of acetic anhydride significantly. In addition, a long reaction time could allow the esterifying agent to react and substitute with the free hydroxyl group of cellulose, resulting in the higher DS value. On the contrary, the decrease in % yield of CLCA and DS at temperature beyond 55 ◦C and extended reaction time above 120 min could be because of cellulose degradation (Ratanakamnuan *et al*., 2012; Fan *et al*., 2013).

The effects of weight ratios of acetic anhydride to cellulose on yield of CLCA are shown in Table 4. Increasing the weight ratio of acetic anhydride to cellulose from 1:5 to 1:8 increased the yield of CLCA as well as DS. However, the weight ratio of acetic anhydride above 1:8 decreased the yield. The accessibly of hydroxyl groups was probably maximal at an acetic anhydride ratio of 1:8 (Nabili *et al*., 2017).

In general, the % yield of CLCA and DS gradually increased with increasing reaction time, temperature and CLC/acetic anhydride, and then decreased after reaching the maximum value. Therefore, the optimum condition for acetylation of CLC were 1:8 CLC/ acetic anhydride at 55 °C for 120 min and 0.2 ml of sulphuric acid providing maximum % yield of CLCA (112.4±1.28%) and DS (2.46) of CLCA.

Table 4: Acetyl content, degree of substitution and yield of CLCA

Reaction condition	CLC/AA ratio (g/ml)	Temperature (^{o}C)	Time (min)	Sulphuric acid (ml)	Acetyl content (%)	DS	Yield (%)
1	1:5	25	30	0.05	18.12	0.83	54.2
2	1:5	40	30	0.05	18.84	0.87	56
3	1:5	55	30	0.05	19.74	0.92	56.8
4	1:5	70	30	0.05	16.48	0.74	52.4
5	1:5	55	60	0.05	20.73	0.98	61.3
6	1:5	55	90	0.05	24.59	1.22	74.9
7	1:5	55	120	0.05	26.54	1.35	76
8	1:5	55	150	0.05	22.70	1.09	67.5
9	1:6	55	120	0.05	28.38	1.48	78
10	1:7	55	120	0.05	34.02	1.92	82.1
11	1:8	55	120	0.05	36.63	2.15	94.6
12	1:9	55	120	0.05	35.41	2.04	86.9
13	1:8	55	120	0.1	38.13	2.29	103.7
14	1:8	55	120	0.2	39.86	2.46	112.4
15	1:8	55	120	0.3	36.95	2.18	83.6

Key - CLC: Cotton linter cellulose, AA: Acetic anhydride, DS: Degree of substitution

In the present study, the yield of CLCA from CLC was 112.4±1.28%. This value is comparable with the result % reported by Barkalow *et al*. (1989) (103 to 150%). However, higher than the yield of CA from cotton linter (54%) reported by Mostafa *et al*. (2015) and from coconut shell (76%) reported by Amaral *et al*. (2019) who used acetic anhydride as an acetylating agent and sulphuric acid as catalysts to obtain CA. This might have been due to the difference in acetylation condition used during the acetylation process and also, the types of cellulosic sources used in the preparation of cellulose acetate.

3.1.5. Degree of polymerization

DP and molecular weight values of CLC and CLCA are presented in Table 5. The isolated cellulose had DP of 472.52±3.64 and molecular weight of about 76,548.24 g/mol. The cellulose isolated from CL showed comparable result with cellulose isolated from cotton gin waste (483.4) by Ibrahim *et al*. (2010) and lower DP than the DP of cellulose samples isolated from rice straw in the range of 532 - 608 and alfa fibers (844) (Ragab *et al*., 2014; Trache *et al*., 2014). The variation of these values largely depends on the sources of cellulose. Also, the isolation method like type and concentration of chemicals used, temperature, and duration of treatment are all determinants for DP of isolated cellulose (Chen *et al*., 2016). However, low DP of the cellulose has a positive aspect for the synthesis of cellulose derivatives, such as cellulose acetate. Since, low DP increases the accessibility to the cellulosic chain improving the yield of the derivation process (Candido and Goncalves, 2016).

The DP and molecular weight values of CLCA DS 2.46 (234.06± 4.12) and 62,091.44 g/mol respectively, were lower than that of CLC. This is probably due to the degradation during acetylation process (Chen *et al*., 2016). However, this value is higher than that of the CLCA DS 0.83 and CCA as shown in Table 5. Also, this value is higher than CA with DS 2.25 from rice straw cellulose (225). This difference may be due to different sources used for acetylation and catalyst used (in case of rice straw, phosphotungstic acid was used as a catalyst) (Fan *et al*., 2013). The other possible reason for increase in DP with increasing DS may be an increase in the hydrodynamic volume by the large number of acetyl groups introduced (Khullar *et al*., 2004).

Table 5: Physico-chemical properties of the CLC, CLCA and CCA

Properties	**CLC**	**CLCA DS 0.83**	**CLCA DS 2.46**	**CCA**
DP	472.52±3.64	148.24±1.80	234.06±4.12	129.82±2.59
M. Wt (g/mol)	76,548.24	29,182.53	62,091.44	33,026.21
pH	7.2±0.03	6.8 ± 0.01	6.5±0.03	6.9± 0.02
Ash value	*	*	0.06	*
Free acid (%)	-	0.05 ±0.19	0.07±0.62	0.03±0.2

Key - CLC: Cotton linter cellulose, CLCA: Cotton linter cellulose acetate, DS: Degree of substitution, CCA: commercial cellulose acetate. * Ash values were not determined.

3.1.6. Solubility of the cellulose acetate

The DS defines molecule solubility in different solvents (Battisti *et al*., 2018). The solubility of CAs in organic solvents is primarily related to their acetyl content. Generally, the solubility of the synthesized CAs in both organic and inorganic solvents is important for their subsequent processing (Bahmid *et al*., 2013; Jogunola *et al*., 2016). A solubility study was conducted to confirm the DS results obtained from titration method. The solubilities of CA in water, acetone and chloroform are given in Table 6.

The results revealed that, the CLCA DS values had a significant effect on the solubility of CA. The samples with DS 0.83 exhibited good solubility in water and no solubility of the sample with 0.83 of DS value was observed in the organic solvent, while the sample with DS 2.46 exhibited good solubility in acetone at ambient temperature. Furthermore, both samples didn't dissolve in chloroform. Since, acetyl groups are more hydrophobic than hydroxyl groups, the replacement of the hydroxyl groups in cellulose with acetyl groups enhance its solubility in organic solvents (Fan *et al*., 2013). In a previous study it was reported that, the CAs with DS value from 2.2 to 2.7 dissolve in acetone and that those with DS value above 2.7 dissolve in chloroform (Cao *et al*., 2010).

Table 6: Solubility test of the CLCA and CCA

Solvent	**CLCA DS 0.83**	**CLCA DS 2.46**	**CCA**
Water	+	–	–
Acetone	–	+	+
Chloroform	–	–	–

Key - CLCA: cotton linter cellulose acetate, CCA: commercial cellulose acetate, DS: degree of substitution. Where: + stands for soluble and – stands for insoluble.

3.1.7. Fourier transforms infrared analysis

FTIR spectroscopy is widely used in cellulose research as it provides a simple method of obtaining direct information on chemical changes that occur during various chemical treatments. In the current study, FTIR spectroscopy was used to determine the functional groups that characterize the CLC and the synthesis of CA. Figure 5 illustrates the FT-IR spectra of CLC, CLCA and CCA.

The FTIR spectra of cellulose sample is described by main bands, with maximum absorbance peaks around 3337, 2896, 1364, 1160, and 1033 cm^{-1}. A strong peak at 3304 cm^{-1} was attributed to the stretch of the hydroxyl group (El Nemr *et al*., 2017). The band observed at 2901 cm^{-1} assigned to asymmetric C–H bands in methyl and methylene groups (Nabili *et al*., 2017) and there is a moisture peak at 1642 cm^{-1} due to an interaction between cellulose and water (Djuned *et al*., 2014). A strong band at 1034 cm^{-1} was attributed to the C–O–C pyranose ring's skeletal vibration (El Nemr *et al*., 2017). Furthermore, the absence of peaks around 1598 cm^{-1} and 1513 cm^{-1} showed the efficient removal of non-cellulosic components from CL (Araujo *et al*., 2020). The two peaks at 1735 cm^{-1} and 1247 cm^{-1} which were attributed to the C=O and C-O out of the plane stretching vibration of the hemicellulose and lignin completely disappeared in the spectra which indicating the isolated CLC are free from hemicellulose and lignin (Rosli *et al*., 2013).

Four major changes were observed in the spectrum of CLCA and CCA as compared to CLC. The decrease of the band in 3304 cm^{-1} is the result of the OH group replacement for the acetyl groups in cellulose structure (Candido *et al*., 2016). However, in case of CLCA DS 0.83 the band in 3304 cm^{-1} was not as such decrease rather it seems native CLC due to its low DS (De Freitas *et al*., 2017). In the spectrum, new peaks appear at 1734 cm^{-1}, 1366 cm^{-1}, and 1217 cm^{-1}, which are attributed to C=O stretching (carbonyl ester), C-H bond at the acetyl [-O (C=O) -CH3] and –CO– stretching (acetate), respectively (Alves *et al*., 2019).

The FTIR spectra of the resultant CLCA with DS 2.46 showed a similar trend to CCA. However, the FTIR of CLCA with DS 2.46 presented the strongest intensity band for the carbonyl group at around 1734 cm^{-1} which coincided with its highest DS in comparison to the CCA (Loo *et al*., 2012). As a further important aspect of successful acetylation, no absorption was observed in the region with measurements 1760 to 1840 cm^{-1} and 1700 cm^{-1} spectra of the acetylated CLC (Das *et al*., 2014; Djuned *et al*., 2014). This indicated that the CLCA are free of un-reacted acetic anhydride and free of acetic acid by-products, respectively.

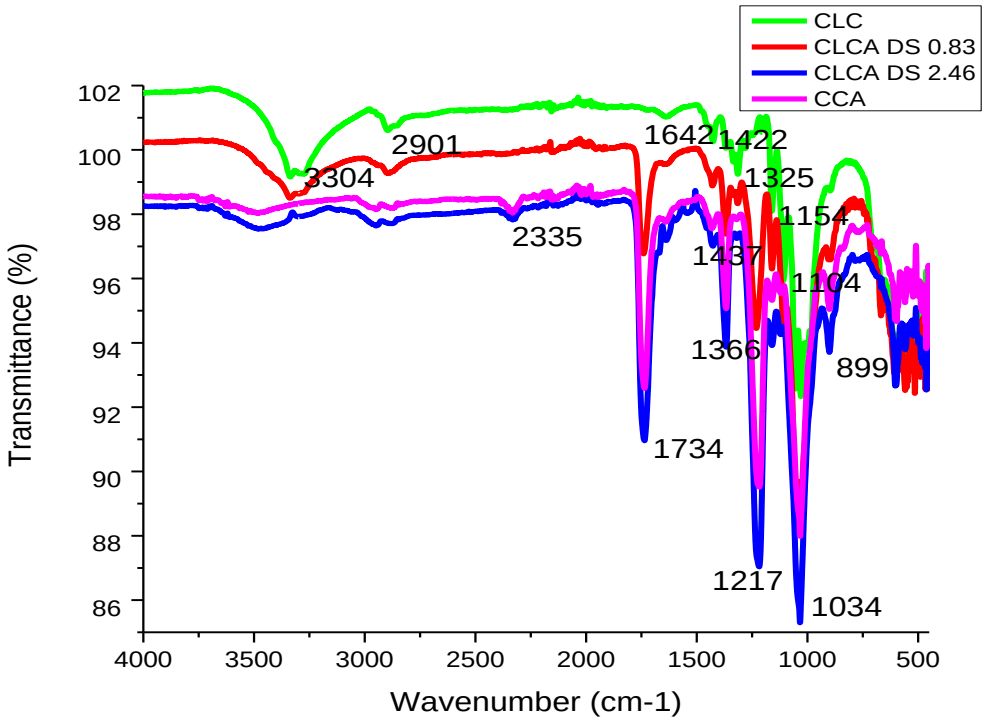

Figure 5: FTIR spectra of CLC, CLCA DS 0.83, CLCA DS 2.46 and CCA.

Key - CLC: cotton linter cellulose, CLCA: cotton linter cellulose, CCA: commercial cellulose acetate, DS: degree of substitution.

3.1.8. X-ray diffraction studies

X-ray diffraction analysis was carried out in order to determine the crystalline and amorphous regions of CLC and CLCA samples. The X-ray diffraction patterns of CLC and its CA are shown in Figure 6. The diffractograms of CLC showed a major peak at 2θ of 14.8, 16.4, 22.67 and 34.5 corresponding to the (1 -10), (110), (002) and (004) diffraction planes respectively, which is characteristic diffraction pattern of cellulose I structure (Oun and Rhim 2015; Chen *et al*., 2016).

Acetylation of the cellulose caused significant changes in the arrangement of the polymer chains of cellulose. X-ray diffraction results indicated that with esterification processing, crystalline structure of native cellulose was destroyed. In comparison to the spectrum of the CLC without acetylation, which shows an intense diffraction peak at 22.67 ◦ the spectra of the CLCAs and CCA showed not obvious peak. However, as can be seen in Figure 6, CLCA DS 0.83 showed a similar profile of CLC. The disappearance of the peak revealed that there was a decrease in crystallinity and a transition of structure from crystalline to amorphous

during the acetylation of the CLC (Loo *et al*., 2012). And this is due to the fact that inter and intra-molecular hydrogen bonds of cellulose were almost completely broken during the substitution of hydroxyl groups by acetyl groups (Chen *et al*., 2016).

The CLCA DS 2.46 and CCA had broad diffraction peak around 2θ = 17◦ is attributed to the less ordered or amorphous region of CA. The diffraction peaks at 2θ of 10.4◦and 13.3◦ are also assigned to the principal characteristic of semi-crystalline region of CA. This resulted by the fact that the substitution of the hydroxyl groups by acetyl groups with greater volume, which broke the inter- and intra-molecular hydrogen bonds of cellulose (Das *et al*., 2014). On the other hand, the XRD patterns of the CLCA with DS 2.46 and CCA are similar. However, CCA has a relatively poorer local order than that of the obtained CA. This result might be associated with the fact that commonly used cellulose diacetate were obtained by hydrolyzing fully substituted CA and the hydrolyzing process might result in the decrease of its crystallinity in case of CCA (Sun *et al*., 2013). The sources of the cellulose used for acetylation may also be another factors.

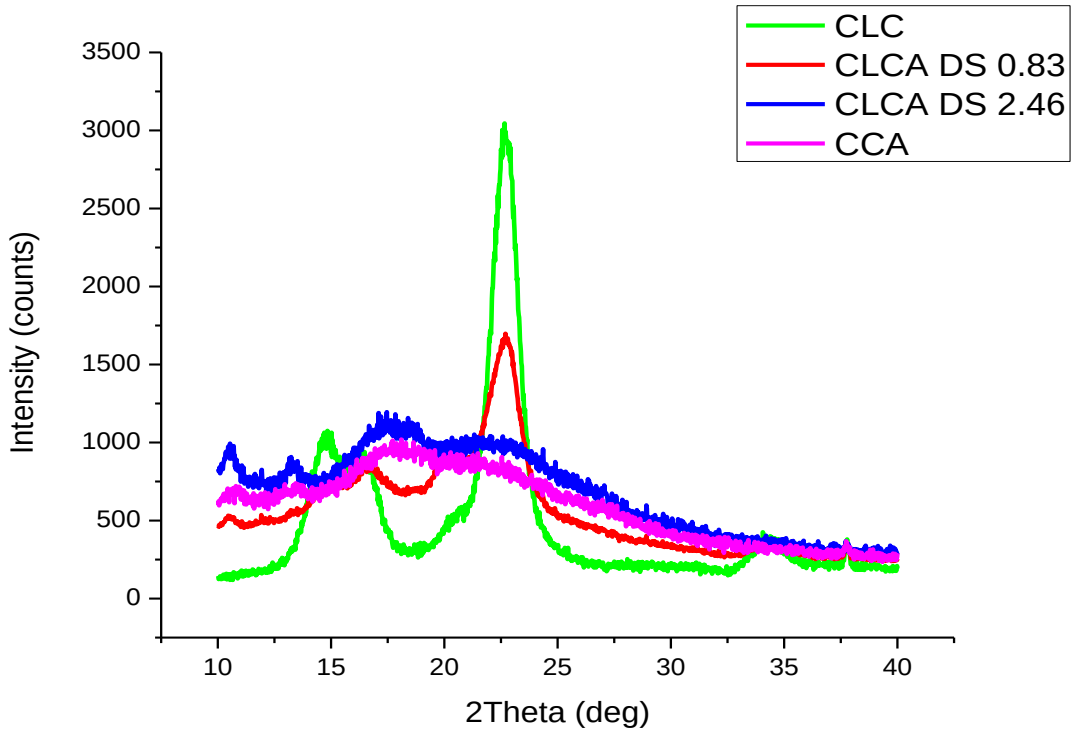

Figure 6: XRD pattern of CLC, CLCA DS 0.83, CLCA DS 2.46 and CCA. (Key- CLC: cotton linter cellulose, CLCA: cotton linter cellulose, CCA: commercial cellulose acetate, DS: degree of substitution).

The crystallinity index of CLC was 81.59 % with high intensity peak, while the amorphous portion causes the background noise line and occurs due to the removal of hemicellulose and lignin molecules (Djuned *et al*., 2014). This value is in agreement with the crystallinity of CLC (80.4%) reported by Seo *et al*. (2013). However, this value is higher than the crystallinity index of cellulose reported by different researchers; CLC (73%) Oun and Rhim, (2015), for Oil palm empty fruit bunches, Corncob and alfa fibers as 70, 44.8 and 59%, respectively (Nazir *et al*., 2013; Zhang *et al*., 2010; Trache *et al*., 2014).

The CLCA produced with a DS 0.83, 2.46 and CCA had lower crystallinity indexes 57.92%, 33.87% and 29.70%, respectively, than CLC. In addition, CLCA DS 2.46 and CCA had lower crystallinity index than corresponding CLCA with DS 0.83, as shown in Table 7, which is consistent with the result reported by De Freitas *et al.* (2017). This indicates that, as the DS of the CA increased, the degree of crystallinity decreased due to an increased destruction or even loss of the ordered crystalline structure.

Table 7: Crystallinity indexes (CrI) of CLC, CLCA DS 0.83, CLCA DS 2.46 and CCA.

Samples	**Peak position at (I_{am})**	**Peak position at (I_{002})**	**%CrI**
CLC	18.86	22.66	81.59
CLCA DS 0.83	18.40	22.65	57.92
CLCADS 2.46	14.44	17.64	33.87
CCA	14.08	17.72	29.70

Key- CLC: cotton linter cellulose, CLCA: cotton linter cellulose, DS: degree of substitution, CCA: commercial cellulose acetate, CrI: crystallinity index.

3.1.9. Morphological characterization

Scanning electron microscopy is a very good instrument to study the diverse morphology of cellulose and its derivatives. The mechanical and physical properties of cellulose depend on the molecular, supramolecular and morphology of cellulose structures (De Freitas *et al*., 2017). Particle morphology is an essential property in the characterization and identification of pharmaceutical excipients.

Figure **7** (A) shows SEM photomicrographs of CLC sample at different size. Morphology of CLC revealed short fiber shapes with smooth surface that were cylindrical with the same size and had perforated layers similar to reports elsewhere (Ratanakamnuan *et al*., 2012; Bahmid

et al., 2013). Figure 7 (B) shows SEM photomicrographs of CLCA DS 2.46 sample at different size. The acetylation of CLC changed the physical appearance of the sample, which are irregular shaped fibrils, course collapsed surface, dense structure with the formation of CA aggregates with a spongy structure, resulting in low surface area and porosity, which are potentially important for its application (El Nemr *et al*., 2017; Alves *et al*., 2019). These results indicated that, the acetyl substitution of acetic anhydride as an acetylating agent led to an aggregation of acetyl substituent groups on the CLC surface (Ratanakamnuan *et al*., 2012).

(A)

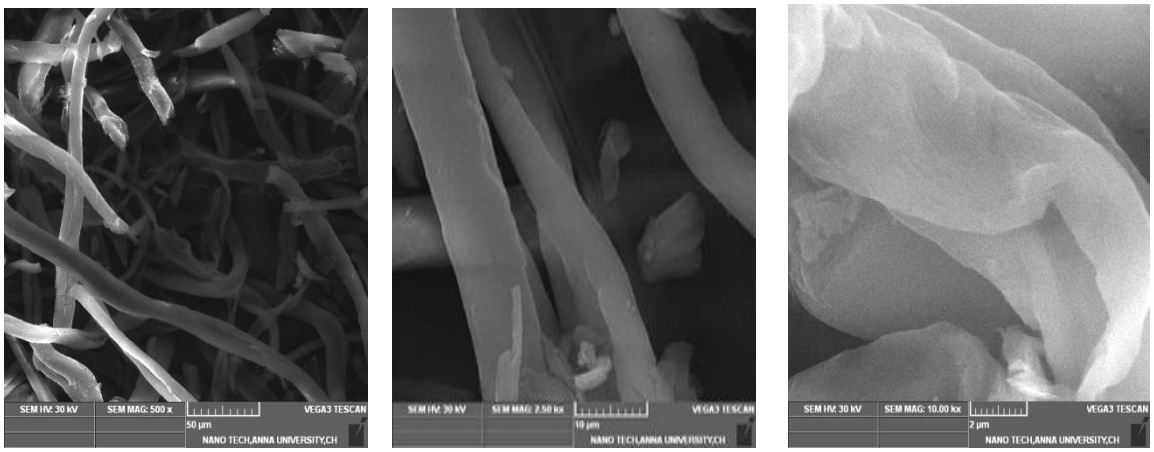

i ii iii

(B)

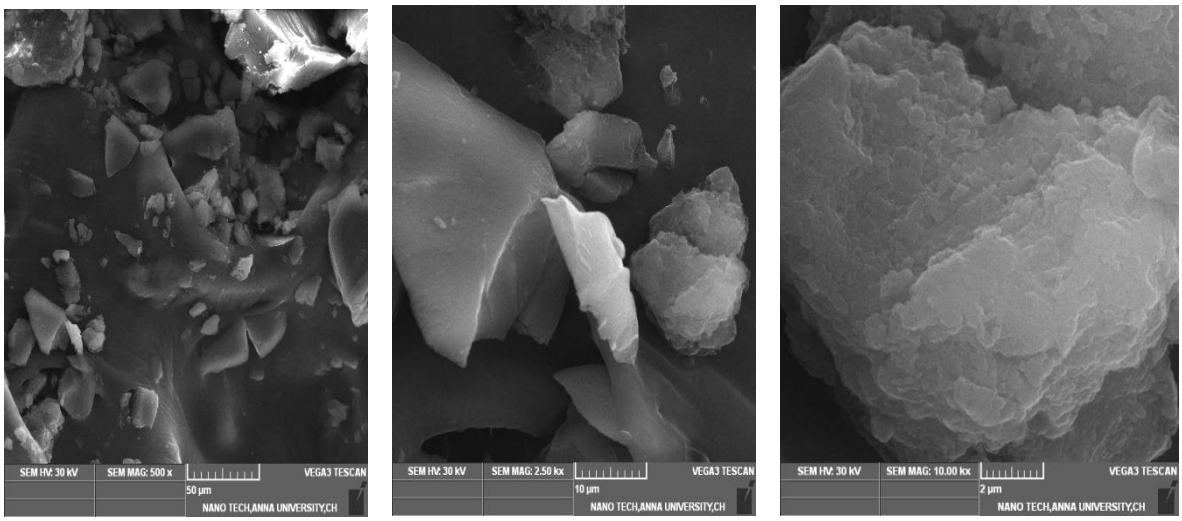

i ii iii

Figure 7: SEM micrographs of the CLC (A) and CLCA DS 2.46 (B) with size of 50 µm (i), 10 µm (ii) and 2 µm (iii).

Key - CLC: Cotton linter cellulose, CLCA: Cotton linter cellulose acetate.

3.1.10. Thermal analysis

Thermogravimetric analysis is a method that can be used to investigate the thermal decomposition due to the formation of volatile product after degradation as a function of temperature (Barbosa *et al*., 2019). It is a convenient, reproducible and useful method for characterizing heterogeneous organic materials. In particular, it is a valuable analytical method to investigate the physico-chemical properties of macromolecules such as cellulose and its derivatives (Ibrahim *et al*., 2010). In order to investigate the thermal properties of the CLC and CLCA samples were characterized by thermogravimetric analysis. Thermograms (TGA and DTG) of CLC, CLCA DS 0.83, CLCA DS 2.46 and CCA are presented below (Figure 8 and 9).

As shown in Figure 8, the thermal properties of the CLC and CLCA DS 0.83 displayed three major weight loss stages with different rate and extent while, CLCA DS 2.46 and CCA exhibited two typical decomposition stages: desorption of water adsorbed in CLC and CLCA DS 0.83 structure and evaporation of volatile compounds, pyrolitic decomposition of polymer chain skeleton followed by deacetylation, and carbonization of degradation products (between 380 and 700°C). From 150 ◦C to 290 ◦C, the TGA curve of CLC and CLCA DS 0.83 displayed a minor weight loss due to the water desorption, which is not obvious in the CA DS 2.46 and CCA (Chen *et al*., 2016). This indicates that the CLCA with high DS (2.46) and CCA samples presented lower water content by the presence of acetyl groups (lower −OH content, which minimizes the water absorption) and this reduces the degradation by hydrolytic cleavage, besides these groups confer greater thermal stability (Barbosa *et al*., 2019).

However, only presence of acetyl group does not determine thermal stability as shown in the thermogram (Figure 8). It was found that CLCA with DS 0.83 has poor stability because first region of weight loss occurred at lower temperature (150 ◦C) as compared to native cellulose (220◦C). The reason may be due to high crystallinity and DP of CLC sample responsible for better thermal stability (Jandura *et al*., 200; Agustin *et al*., 2015). It is instructive that thermal stability of high DS acetylated cellulose is much better than that of the CLC when DS reached to 2.46, the intensity of the first weight loss almost disappeared.

The onset and end thermal degradation temperature of CLC and CLCA DS 0.83 are lower than those of the CLCA DS 2.46 and CCA, and similarly the maximum weight loss rate peak

of CLCA DS 0.83 is also lower than that of the CLCA DS 2.46 and CCA. In case of CLCA DS 2.46 and CCA the onset temperature (Tonset) are almost similar (T onset =321 ◦C, 324 ◦C), respectively and end (Tend) temperature samples are similar (400 ◦C) as shown in Figure 8. These results show that the thermal stability of synthesized CLCA DS 2.46 and CCA samples are very similar and they reveal higher thermal stability than the CLC and CLCA DS 0.83. This is in agreement with the data reported by Chen *et al*. (2016).

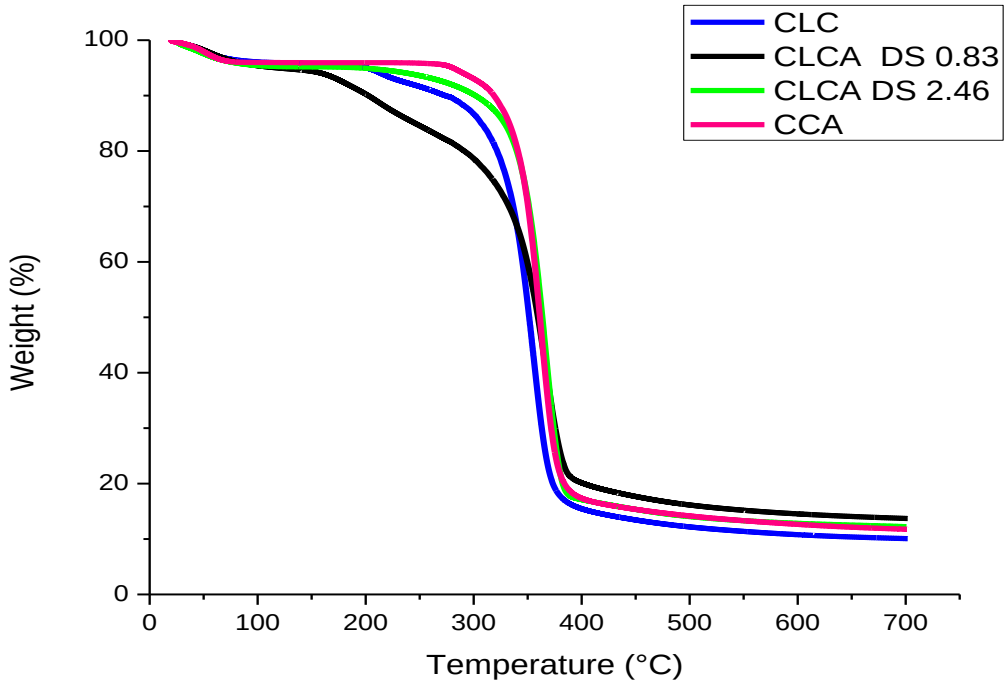

Figure 8: TGA thermograms of CLC, CLCA DS 0.83, CLCA DS 2.46 and CCA samples. Key - CLC: cotton linter cellulose, CLCA: cotton linter cellulose acetate, CCA: commercial cellulose acetate, DS: degree of substitution.

Generally, the thermal properties of cellulose derivatives are sensitive to DS changes. It has been reported that the thermal stability of CA increases with DS and molecular weight (Barud *et al*., 2008; Chen *et al*., 2016). This can be explained by the fact that, as DS increases, more acetyl groups are introduced onto the C2 and C3 carbons of the AGU, which require more energy when compared to the least sterically hindered group C6COOCH3, and increase the apparent activation energy for thermal decomposition, leading to an increase in thermal stability (Araujo *et al.*, 2020). The increase in thermal stability at high DS can be also attributed to the possible inhibition of inter- and intra-molecular hydrogen bond formation

when the OH groups are substituted with acetyl groups and low amount of remaining hydroxyl groups after acetylation (Agustin *et al*., 2015; Zhang *et al*., 2009). These results also confirm that the thermal stability of the CLCA increased with DS from 0.83 to 2.46.

DTG was used to measure the occurrence of exothermal or endothermal changes with increase in temperature (Zhang *et al*., 2009). The DTG curves of the CLC, CLCA DS 0.83, DS 2.46 and CCA samples are shown in Figure 9. Two endotherms emerges in the DTG curve of CLC and CLCA DS 0.83. The first, one is a minor one is caused by the decomposition of samples, the other one is due to the decomposition of substituted (peak temperature ◦C). In the case of CLCA DS 2.46 and CLCA, there is an obvious endothermic peak occurs at higher temperature (peak temperature ◦C) as compared to CLC and CLCA DS 0.83.

The DTG result also confirm that the maximum degradation rate of the CLCA DS 2.46 and CCA appeared at higher temperature than that of CLC, indicating that the thermal properties of the synthesized CA were slightly improved by introducing the acetyl group into cellulose. In addition, the thermal stability increased with increasing DS, in accordance with TGA result (Wang *et al*., 2017).

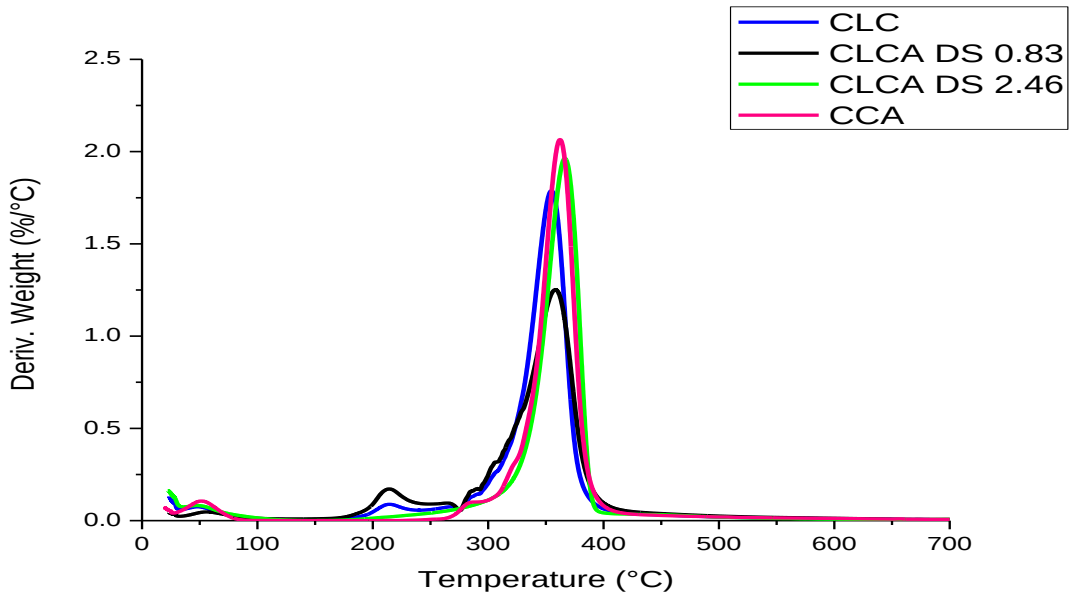

Figure 9: DTG thermograms of CLC, CLCA DS 0.83, CLCA DS 2.46 and CCA samples. Key - CLC: cotton linter cellulose, CLCA: cotton linter cellulose acetate, CCA: commercial cellulose acetate, DS: degree of substitution.

3.2. Powder properties of the Cellulose Acetate

3.2.1. Density and other related properties

The powder properties of the CLCA, CCA and EC were evaluated for various pre-compressional parameters such as bulk density, tapped density, true density, compressibility index, Hausner's ratio, angle of repose and flow rate as shown Table 8. The bulk density of a powder describes its packing behavior while the tapped density indicates the rate and extent of packing that would be experienced by a material during the various unit operations of tableting (Zuliahani *et al*., 2016). Bulk and tap densities values are good, since they are within the following ranges 0.35±0.06 to 0.41±0.04 and 0.42±0.03 to 0.48±0.04g ml^{-1}, respectively. The values of the bulk and tapped densities provide information on the flowability of powders and are used to calculate the Carr's index (CI) and Hausner ratio (HR), which are a measure of the flowability and compressibility of a powder (USP38/NF33, 2015).

Flow is an important property in tablet production, because an adequate level of powder flow is needed to ensure a constant fill of the tablet die during production (Nagel and Peck 2003). The Hausner ratio for CLCA DS 2.46, CCA and EC is less than 1.2 which indicates good flowability. The range of compressibility index was 11.63±1.87 to 14.58±1.33 indicating good compressibility as these parameters of all powders are within the USP range of powders with good flow properties/ good compressibility (USP, 2012). On the other hand, as DS of CLCA increased, flow property improved significantly, that is the Hausner ratio and compressibility index of CLCA DS 2.46 value reduced when compared with CLCA DS 0.83 as shown in Table 8. In case of CLCA DS 0.83, the Hausner ratio is 1.26 ± 0.07 and the compressibility index is 20.45 ± 3.52.This values indicate poor flow properties of CLCA DS 0.83 (USP, 2012).

The angle of repose is another qualitative measure of the cohesiveness or the tendency of powdered materials to flow. The angles of repose of CLCA DS 2.46, CCA and EC were 27.28±1.32, 25.17±2.26 and 24.48±2.15, respectively. The results for angle of repose < 30 indicate good flow properties of the powder. This was further supported by lower compressibility index and Hausner's ratio values of those samples as shown in Table 8. The angle of repose of CLCA DS 0.83 was 31.16±3.04. This value indicates poor flow property.

Therefore, to improve the flow property of CA DS 0.83 powder, 0.5 % magnesium stearate was added.

Moisture content affects manufacturing of the solid formulation. Higher moisture content can result in poor powder flow, which could further result in irregular tablet parameter performance. It may also result in sticking problems on the surface of the tableting machine (Tomar *et al*., 2017). The moisture content of CLCA found to be suitable for direct compression formulation and CLCA with DS 2.46 showed comparable result with CCA as show in Table 8. Generally, the optimal moisture content (3.37±0.18) and favourable powder flow property of CLCA DS 2.46 make it suitable for direct compression formulations.

Table 8: Powder properties of CLCA DS 0.83, CLCA DS2.46, CCA and EC (mean ±SD).

Powder properties	**Samples**			
	CLCA DS 0.83	**CLCA DS 2.46**	**CCA**	**EC**
Bulk density (g/ml)	0.35±0.06	0.41±0.04	0.38±0.02	0.37± 0.01
Tapped density (g/ml)	0.44±0.04	0.48±0.03	0.43±0.05	0.42±0.02
True density (g/ml)	1.34±0.03	1.3±0.05	1.27±0.04	*
Hausner's ratio	1.26±0.04	1.17±0.05	1.13±0.03	1.14±0.04
Carr's index (%)	20.45±3.52	14.58±1.33	11.63±1.87	11.90±1.47
Angle of repose (°)	31.16±3.04	27.28±1.32	25.17±2.26	24.48±2.15
Flow rate (g/sec)	6.91± 1.54	5.04± 0.69	4.82±1.21	4.06± 0.73
Moisture content	4.26± 0.09	3.37±0.18	3.51±0.13	*

Key - CLCA: cotton linter cellulose acetate, CCA: commercial cellulose acetate, DS: degree of substitution, EC: Ethyl cellulose

* The moisture content and true density of the EC were not determined

3.2.2. Moisture sorption pattern

A water sorption isotherm reflects the interaction between a powder material and water by relating the humidity of air in equilibrium with water content of the solid material at a constant temperature (Puncochová *et al*., 2011). The evaluation of water sorption profiles of pharmaceutical excipients is of utmost importance for a suitable formulation of solid dosage forms. Chemical stability and physical properties of the formulation can be changed if

too much water is bound due to water sorption ability of the powders (Roskar and Kmetec, 2005). The moisture sorption profiles of CLCA DS 0.83, CLCA DS 2.46 and CCA are depicted in Figure 10.

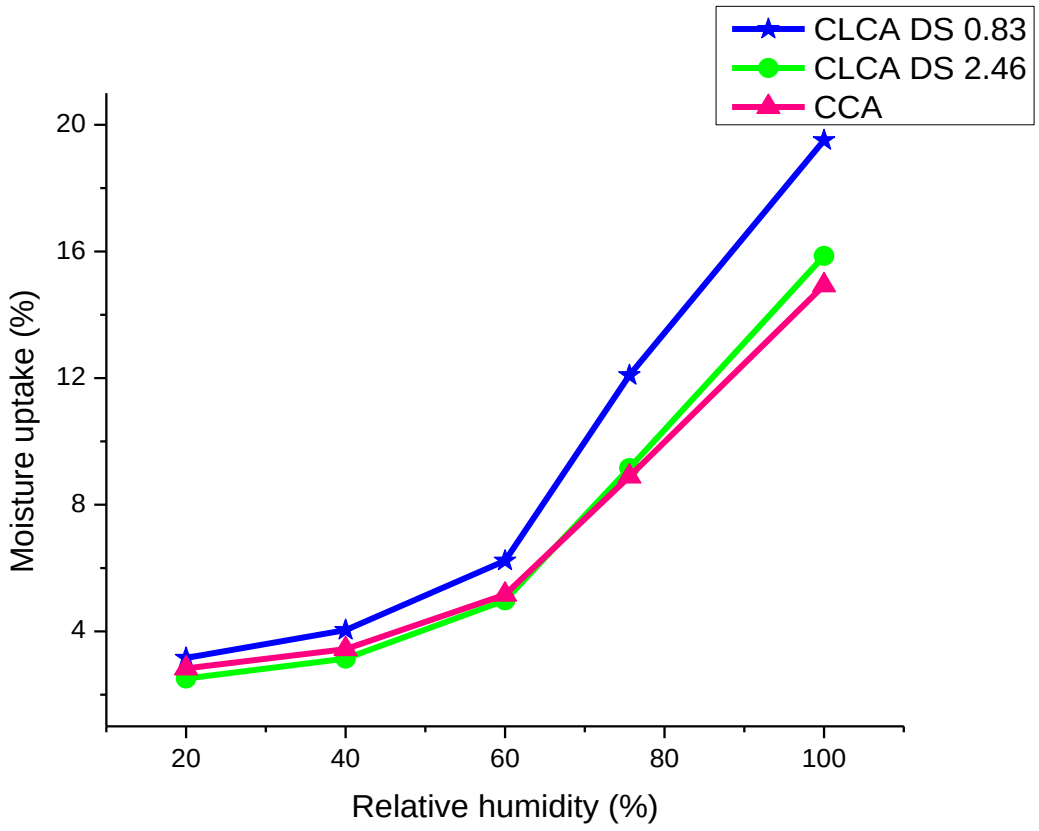

Figure 10: Moisture sorption patterns of CLCA DS 0.83, CLCA DS 2.46 and CCA at various RHs and room temperature. (Key - CLCA: cotton linter cellulose acetate, CCA: commercial cellulose acetate, DS: degree of substitution).

As can be seen in the above Figure, the moisture uptake of CLCA and CCA powders slightly increased with RH at lower values but increased significantly above 60% relative humidity. The CLCA DS 0.83 had the highest moisture uptake when compared with CLCA DS 2.46 and CCA. This might have resulted from their low DS due to higher surface area and more accessible hydroxyl groups. In contrast, the decrease in the surface area and hydroxyl groups at higher DS powder hydrophobicity is developed. This implies that at higher DS, when more hydroxyl groups are substituted by acetyl groups, moisture sorption is reduced (Asaadi *et al*., 2018).

3.2.3. Kawakita analysis result

The method of direct compression involves compressing ingredients into tablets at suitable compression pressure. It is therefore necessary to evaluate the compaction behaviour of excipients, because the compaction behavior determines the tabletability of the formulation (Haruna *et al*., 2020). Compressibility and cohesiveness can be further confirmed by Kawakita constants that indicate the behavior of the powder from the bulk density to the tapped density state. The constants of the Kawakita equation were computed from the slope and intercept of the line from the graph N/C versus N. Constants „a" (compressibility, or the amount of densification due to tapping) and „1/b" (cohesiveness, or how fast or easily the final packing state was achieved), indicating good flow ability and small cohesiveness (Vaidya and Avachat, 2011; Ohwoavworhua *et al*., 2007).

Kawakita plots presenting the compaction profiles of CLCA DS 0.83, CLCA DS 2.46, CCA and EC are displayed in Figure 11. As shown in Figure 11 the Kawakita plots of CLCA DS 0.83, CLCA DS 2.46, CCA and EC resulted in a linear relationship with equations of Y = 5.6505X + 18.371, Y = 8.9692X + 40.306, Y = 8.5774x +70.916 and Y = 9.143X+66.848 respectively, where Y is N/C and X is N.

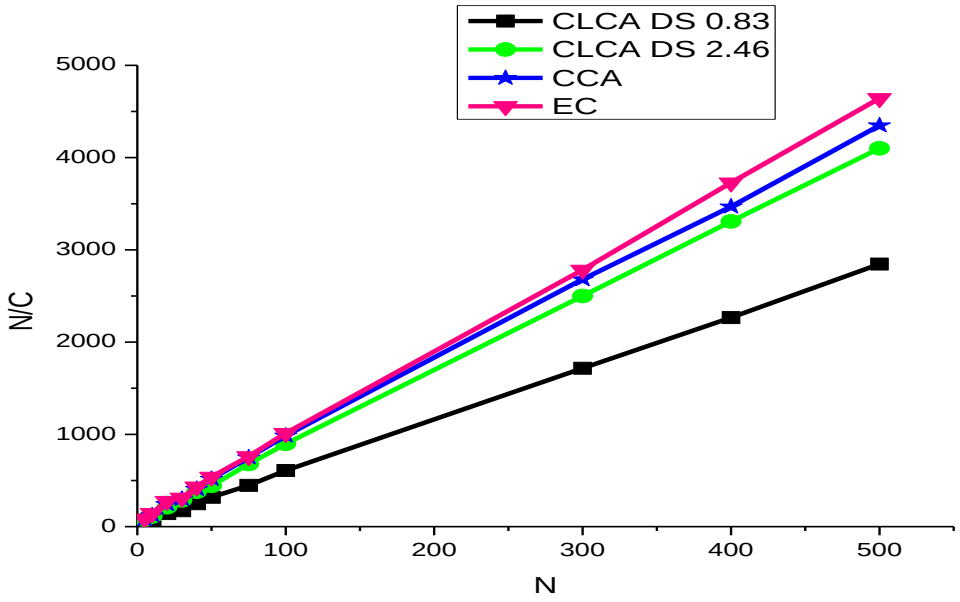

Figure 11: Kawakita plots of CLCA DS 0.83, CLCA 2.46, CCA and EC. (Key - CLCA: cotton linter cellulose acetate, DS: degree of substitution, CCA: commercial cellulose acetate, EC: Ethyl cellulose).

The results of powder densification study presented in Table 9 showed that CLCA DS 2.46, CCA and EC densified the least (due to small compressibility values) and attained the final packing state slowly (the greater cohesive values), indicating good flowability which is necessary for direct compression tableting. On the other hand, CLCA DS 0.83 densified considerably and was the fastest to attain the final packing state. The Kawakita analysis supported the fact that the high DS of CLCA (2.46) improves the powder flowability. Therefore, the smaller 'a' values of CLCA DS 2.46, CCA and EC indicate good flowability.

Table 9: Kawakita constants of CLCA DS 0.83, CLCA DS 2.46, CCA and EC.

Samples	**Kawakita compressibility (a)**	**Kawakita cohesiveness (1/b)**	**Correlation coefficient (R^2)**
CLCA DS 0.83	0.177	3.251	0.9998
CLCA DS 2.46	0.123	6.024	0.9999
CCA	0.117	8.268	0.9997
EC	0.109	7.172	0.9998

Key - CLCA: cotton linter cellulose acetate, DS: degree of substitution, CCA: commercial cellulose acetate, EC: Ethyl cellulose

3.3. Drug-Excipient Compatibility Study

Compatibility study of drug and CLCA were conducted by FTIR Spectral studies. The FTIR spectra of pure theophylline, physical mixture (1:1) of theophylline and CLCA are displayed in Figure 12. The following characteristic peaks were observed with pure theophylline as well as physical mixture of the theophylline and CLCA: The band around 1706 cm^{-1} is characteristic of the imide stretching of the heterocyclic moiety. A peak around 1664 cm^{-1} is due to tertiary amide group stretching vibrations. The N-H bending vibration is shown at 1563 cm^{-1}, whereas C-H - (stretching) at 3127 cm^{-1} (Masareddy *et al*., 2012). The peak observed from FTIR studies showed that there is no appearance or disappearance of any characteristic peaks observed in the physical mixture of the theophylline and CLCA which indicates the absence of chemical interaction between drug and CLCA sample thereby showing compatibility between the samples.

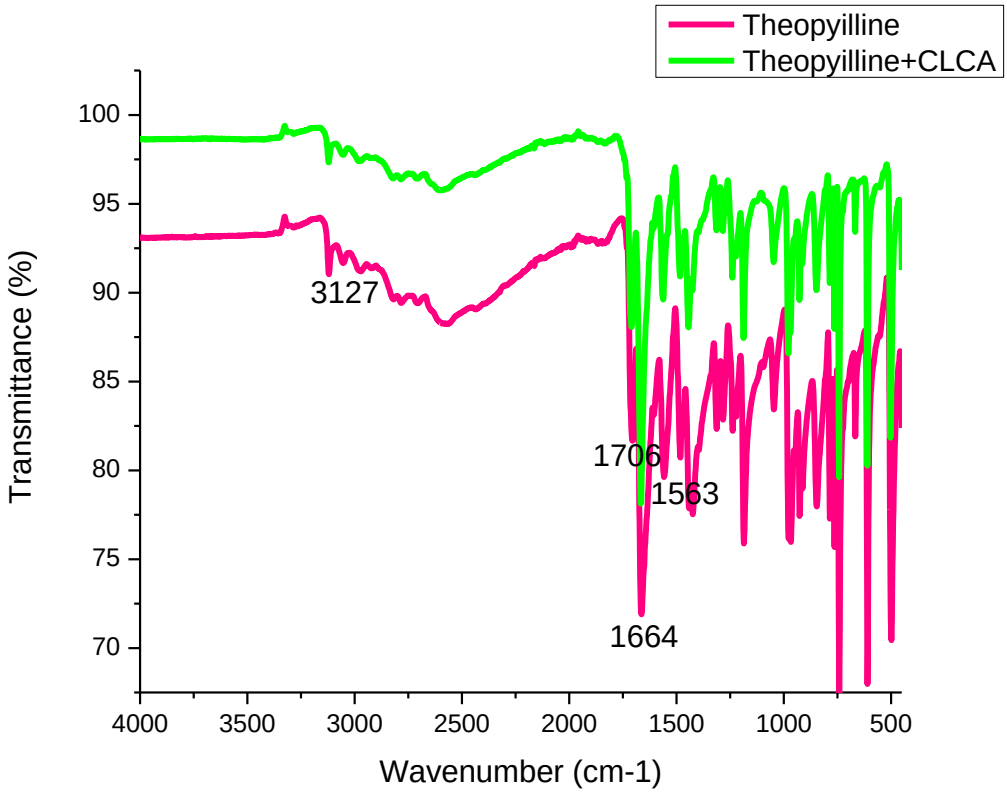

Figure 12: FTIR spectrum of pure theophylline and physical mixture of theophylline and CLCA (cotton linter cellulose acetate).

3.4. Characteristics of Tablets

The crushing strength, friability, tensile strength, porosity and disintegration time of plain tablets are shown in Table 10. Plain CLCA DS 2.46 showed improved compression than the CLCA DS 0.83 and comparable result with CCA and EC resulting in higher crushing strength. As the degree of acetylation increases, polymer turns more hydrophobic, then the mechanical strength increases and disintegration does not occur any more (Raatikainen *et al*., 2002).

Friability measure the physical strength of the tablet. A maximum weight loss of not more than 1.0% is generally considered acceptable (USP38/NF33, 2015). The friability of the plain tablets were found within range of (0.14 % to 0.92 %). However, plain tablets of CLCA DS 0.83 had larger weight losses than CLCA DS 2.46, CCA and EC samples showed smaller weight losses during the friability test as shown in Table 10.

In disintegration tests, plain tablets of CLCA DS 0.83 were completely disintegrated within a 20 min while tablets made of plain CLCA DS 2.46, CCA and EC did not disintegrate at all within 2 h. It was clear that the manufactured tablets exhibit acceptable properties in terms of weight uniformity, diameter, thickness, crushing strength, and friability at the studied tablet hardness. The plain tablets of CLCA DS 2.46 showed high tensile strength and lower porosity than CLCA DS 0.83 and comparable result with CCA but slightly differ with EC (Table 10).

3.4.1. Crushing strength and friability

As shown in Table 11, the hardness of the tablets of all batches ranged from 131.2±8.81 162.9±7.92 N. Tablets prepared from CLCA with DS 0.83 (F4) had the low crushing strength than all batches. Tablets prepared from high concentration of CLCA DS 2.46 (F1) had a higher crushing strength than those tablets prepared with low concentration of the CLCA DS 2.46 (F2 and F3). The low hardness values observed with formulations F2 and F3 might be due to the presence of low levels of CLCA in the tablets. These results were in close agreement with those reported by Subhedar *et al*. (2010). They confirmed that hardness of the tablet increases with increase in polymer concentration in the tablet which can significantly affect mechanical properties that are considered as an important quality attribute of the hydrophobic matrix tablets.

The friability profiles of the tablets are in line with the crushing strength measurements as shown in Table 11. Tablets made from CLCA DS 0.83 exhibited higher friability (0.89%) than tablets made from CLCA DS 2.46, CCA and EC. However, the friability values were less than 1% in all formulations indicating that the formulated tablets were mechanically stable and meet the pharmacopoeial requirements (USP38/NF33, 2015). As shown in Table 11, the friability of the matrix tablets of CLCA DS 2.46 increased as the percentage of anhydrous theophylline increased from 20% to 30% and 40% (w/w) due to reduced crushing strength of CLCA DS 2.46 tablets containing 40% (w/w) theophylline. In general, increase in tablet crushing strength results in lower friability values and longer disintegration times.

3.4.2. Tensile strength

The measurement of tensile strengths provides a more fundamental measure of the mechanical strength of the compacted material and the ability of particle binding (USP38/NF33, 2015). As shown in Table 11, the tensile strength of the tablets of all batches ranged from 15.28±1.26 to 28.64±1.34 Kg/cm^2 indicating good mechanical strength. The

tensile strengths of tablets prepared from CLCA DS 2.46 were higher than tablets prepared from the CLCA DS 0.83 and showed comparable to those of CCA. The increase in tensile strength is attributed to the increase in compactibility of the CLCA DS 2.46. However, the tensile strength of tablets prepared from CLCA DS 2.46 was lower than EC containing formulation (F6). In addition, as concentration of CLCA DS 2.46 increases (F3 to F1), the tensile strength of the tablets also increased as shown in Table 11. Studies by Rao *et al*. (2016) also showed that the tensile strength of a tablet increases with increasing polymer concentration ratio.

3.4.3. Porosity

For a hydrophobic matrix tablet, irregular pores will be formed during compression due to the boundaries of the particles. The release rate of a drug from hydrophobic matrix can be modified by changes in the porosity and tortuosity of the matrix, because of pore structure, size and number of the pores in the formulation preceded by drug dissolution in the water-filled pores and by diffusion through the water-filled channels (Peppas, 1983).

As shown in Table 11, the porosity of tablet matrix containing CLCA DS 2.46 decreased as compared to CLCA DS 0.83 containing formulation. This showed that, fewer diffusion channels may be presented due to the decreased porosity in case of CLCA DS 2.46. Consequently, slower drug release profile was observed for CLCA DS 2.46 than CLCA DS 0.83, as shown Figure 15. In addition, the porosity of tablet also affected by concentration of polymer used as shown in Table 11. As CLCA DS 2.46 concentration increases, the porosity of matrix tablets decreased. Generally, this result suggests that porosity is one factor influencing on the drug dissolution in addition to other factors.

3.4.4. Disintegration test

Matrix tablets made from CLCA DS 2.46, CCA and EC took longer time to disintegrate as compared to tablets which were made from CLCA DS 0.83. Generally the disintegration time are related to hardness. When the hardness increased, the disintegration time increased. As shown in Table 11, tablets made from CLCA DS 0.83 (F4) exhibited short disintegration time (32 min) than those tablets prepared with CLCA DS 2.46 (F1, F2, F3), CCA (F5) and EC (F6) showed a disintegration times of longer than 2 h. The reason may be due to that, as hardness increased there was more compactibility in the tablets containing CLCA DS 2.46, CCA and EC and it takes longer time to disintegrate.

Table 10: The weight, thickness, diameter, crushing strength, friability, tensile strength, porosity and disintegration time of plain tablets (mean ±SD).

Parameters	**Formulations**			
	CLCA DS 0.83	**CLCA DS 2.46**	**CCA**	**EC**
Weight (mg)	401.07±5.32	399.26±6.80	397.5±3.29	398.13±4.87
Thickness (mm)	4.68±0.17	4.54±0.08	4.47±0.13	4.61±0.22
Diameter (mm)	10.89±0.04	10.78±0.09	10.82±0.05	10.85±0.03
Crushing strength (N)	124.4±9.78	151.2±10.13	148.34±8.64	159.3±7.21
Tensile strength (Kg/cm^2)	16.36±1.94	24.58±2.45	21.01± 3.2	27.3±1.42
Friability (%)	0.92	0.31	0.26	0.14
Porosity (%)	18.31±1.54	9.27±2.03	10.14± 1.92	*
Disintegration time (min)	20	>120	>120	>120

Key - CCA: commercial cellulose acetate, CLCA: cotton linter cellulose acetate, DS: degree of substitution, EC: Ethyl cellulose.

* The porosity of the EC was not determined

Table 11: The weight, thickness, diameter, crushing strength, friability, tensile strength, porosity, disintegration time of matrix tablets used for drug release studies (mean ±SD).

Parameters	**Formulations**					
	F1	**F2**	**F3**	**F4**	**F5**	**F6**
Weight (mg)	400.75±4.38	398.25±8.61	399.60±3.91	397±7.36	399±5.23	401.05±4.08
Thickness (mm)	4.76±0.16	4.68±0.09	4.57±0.14	4.43±0.16	4.63± 0.8	4.81±0.13
Diameter (mm)	10.91±0.04	10.82±0.08	10.86±0.05	10.83+0.03	11.02± 0.05	10.88±0.03
Crushing strength (N)	158.4±6.79	147.5±9.18	143±8.64	131.2±8.81	152.7± 4.31	162.9±7.92
Tensile strength (Kg/cm^2)	23.31±0.72	20.89±1.13	19.47±0.98	15.28±1.26	20.06±1.81	28.64±1.34
Friability (%)	0.29	0.44	0.68	0.89	0.37	0.09
Porosity (%)	10.34± 1.27	12.86± 0.08	15.04± 0.9	23.4± 1.03	12. 97± 1.07	*
Disintegration time (min)	>120	>120	>120	32	>120	>120

* Porosity of F6 was not determined

3.4.5. UV calibration curve of theophylline

From stock solution of 50 µg/ml of theophylline in 0.1 N HCl and phosphate buffer (pH 6.8), the calibration curve was plotted at seven different concentrations (µg/ml). The absorbance (at 271 nm) versus concentration of the solutions was plotted and a calibration curve with a linear regression equation of Y = 0.07315X - 0.01814(R^2 = 0.9996) and Y=0.06641X - 0.00423 (R^2 =0.9998) in 0.1N HCl and phosphate buffer (pH 6.8) were obtained, respectively (where Y is the absorbance and X is the concentration in µg/ml) (Figure 13 and 14).

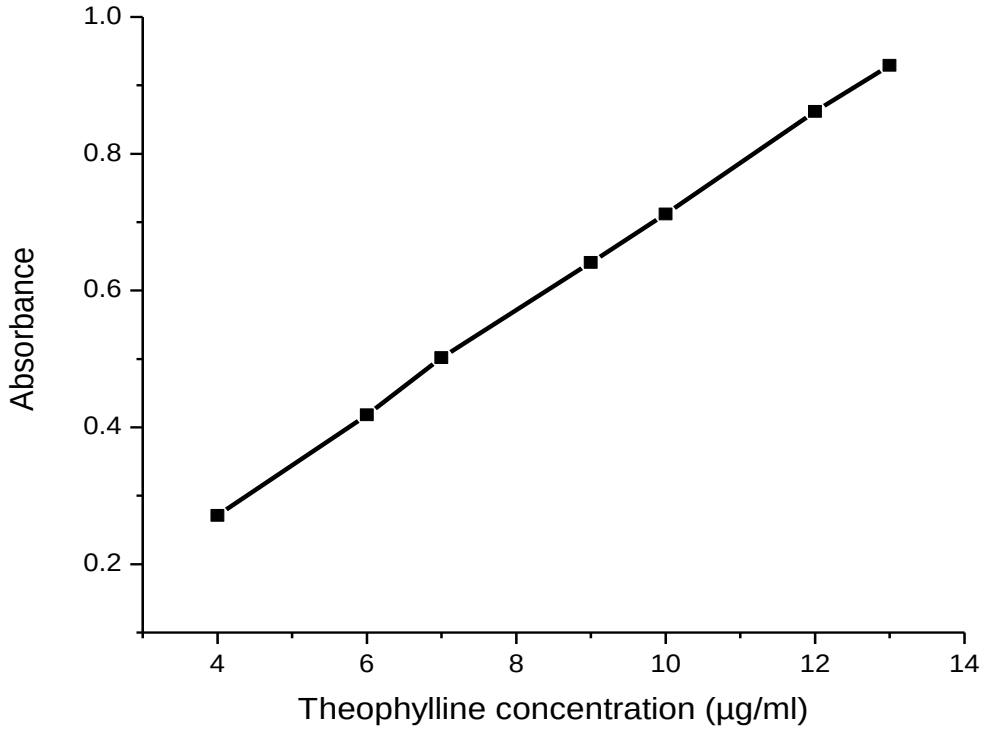

Figure 13: Standard calibration curve of theophylline in 0.1 N HCl solutions at 271 nm with 95% confidence bands for the mean; (R^2 = 0.9996).

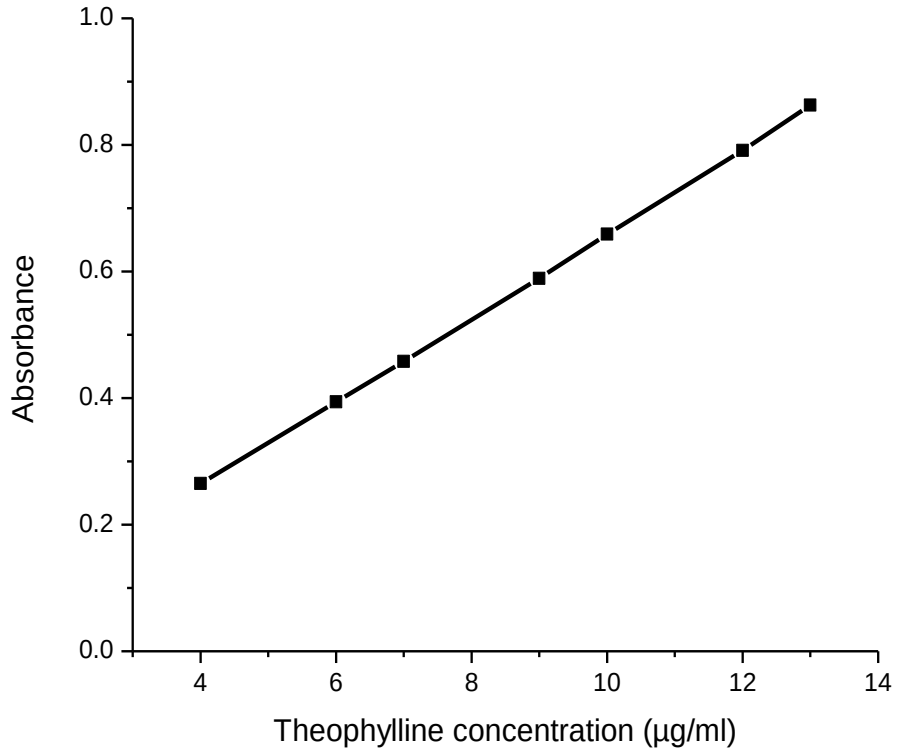

Figure 14: Standard calibration curve of theophylline in phosphate buffer (pH = 6.8) solution at 271 nm with 95% confidence bands for the mean; (R^2 = 0.9998).

3.4.6. *In vitro* drug release test

Dissolution studies were performed in 0.1 N HCl for the first 2 h and in phosphate buffer solution (pH 6.8) for the remaining 10 h. The dissolution profiles of theophylline from CLCA DS 2.46, CLCA DS 0.83, CCA and EC tablets are depicted in Figure 15.

A higher percentage of drug release was observed from the tablets with CLCA DS 0.83 (F4) as compared with CLCA DS 2.46 based tablets (F1-F3), CCA (F5) and EC based tablet (F6). Almost 100% of drug was released within a few h and therefore CLCA DS 0.83 had no SR property. This might be due to higher porosity of tablets which can enhance drug release. As can be seen from Figure 15, the dissolution rate of theophylline changed from rapid release to SR as the DS increased from 0.83 to 2.46, indicating that DS of the CLCA had a significant effect on drug release from the tablets. The release was more sustained from the tablets incorporated with CLCA of higher DS (2.46). As the DS of the CLCA increases, more time is required for the drug to be released from the matrices into the medium. Longer release times

from the CLCA DS 2.46 formulations can probably be explained by a limited water access into matrix due to the high hydrophobic character contributed by the increased acetyl moieties than CLCA DS 0.83.

As seen in Figure 15, the drug release from F1 (CLCA DS 2.46) and F5 (CCA) matrices containing 20% (w/w) of theophylline showed comparable results, while tablet with EC containing 20 % (w/w) of theophylline had more sustained release effect than CLCA DS 2.46 and CCA. This difference may be due to EC containing tablet had higher crushing strength (162.9 N) and tensile strength than both excipients (CLCA DS 2.46 and CCA) as observed in Table 11. As result reduction in the porosity of the matrices and simultaneous increase in matrix tortuosity owing to the formation of continuous matrix at higher crushing strength leading to slower water uptake and water front movement into the matrix, which in turn, may lead to slower drug release (Quadir *et al*., 2005; Vaidya and Avachat, 2011). Further, EC is more hydrophobic than the CLCAs and hence less penetration of the dissolution medium into the tablets containing EC (F6).

The concentration of the polymer in the matrix tablet is a key factor in maintaining the drug release (Rao *et al*., 2016). In order to investigate the effect of polymer concentration on drug release profile, different formulations containing various percentages of CLCA DS 2.46 were used. From the release profiles, it can be observed that polymer-to-drug ratio affected the release rate of the matrices. As shown in Figure 15, the drug released from formulation F1 to F3 containing CLCA DS 2.46 at three concentration levels of 79.5%, 69.5% and 59.5% were found to be 51.63 %, 67.29 % and 84.34 %, respectively, at the end of 12 h.

These results indicate that the higher polymeric content in the matrix reduces the release rate of drug. The study done by Reza *et al*. (2003) also confirm that as polymer concentration increase the drug release rate from matrix was reduced. This can be explained by the fact that an increase in polymer content results in decreased drug release rate due to a decrease in the porosity of the matrix. The increase in polymer content also increases the tortuosity of the matrix and the length of the drug diffusion path, thereby slowing down the diffusion and erosion from the matrix (Quadir *et al*., 2003). In addition as polymer/drug ratio increases, the polymeric phase became more viscous, which in turn strongly shield the drug and hinder the diffusion of the dissolution medium into matrix tablet to dissolve the drug as well as the diffusion of the dissolved drug out of the matrix (Sahoo *et al*., 2011).

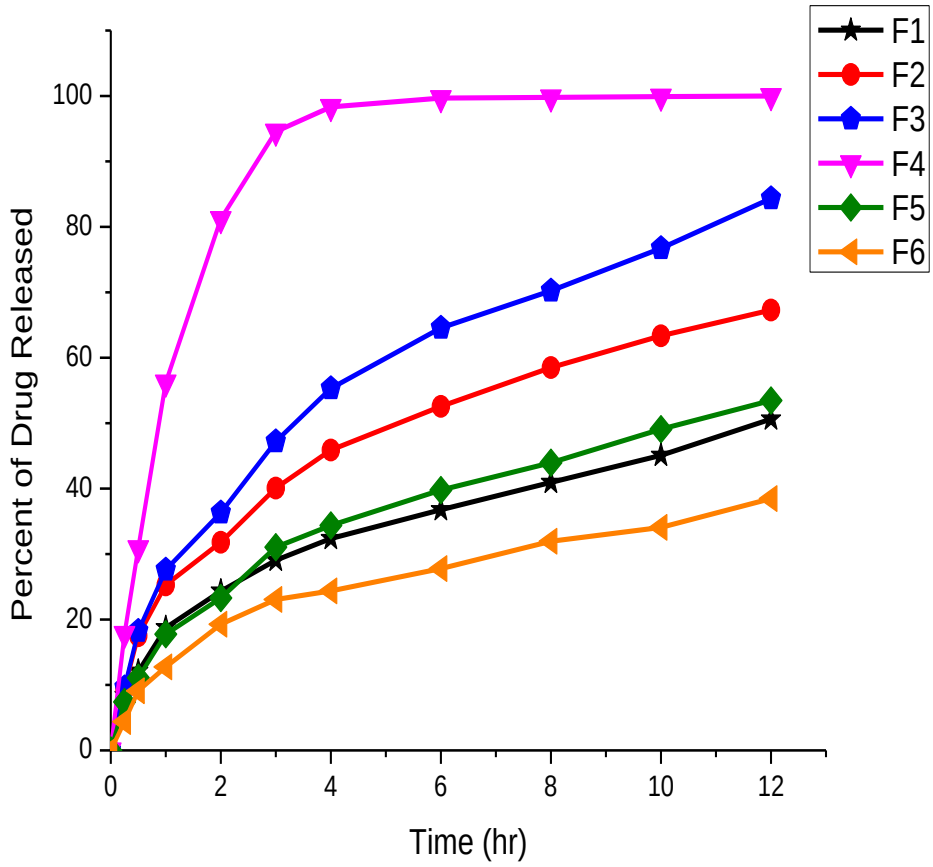

Figure 15: Release of theophylline from CLCA DS 2.46 tablets (400mg) containing 20%, 30% and 40% drug and 20% drug with CLCA DS 0.83, CCA and EC.

Key - CLCA: cotton linter cellulose acetate, CCA: commercial cellulose acetate, DS: degree of substitution, EC: Ethyl cellulose

3.5. Drug Release Kinetics

The drug release kinetic is directed by one or more mechanisms that depend on the composition of the matrix, geometry, preparation method and dissolution medium. Drug release from matrix tablets, in general, becomes progressively slower with time, like Higuchi's model, in which the amount of drug released is proportional to the square root of time. Kinetic models which fit zero order and Higuchi are more suitable for controlled release formulations (Ojoe *et al*., 2005). Therefore, to understand the drug release mechanism; the data were fitted to different models. The drug release data obtained were extrapolated by Zero order, First order, Higuchi, Korsmeyer-Peppas and Hixson Crowell equations as shown

Figure 16. The drug release constant (k), regression coefficient (R^2) and release exponent (n) obtained from these models are shown in Table 12.

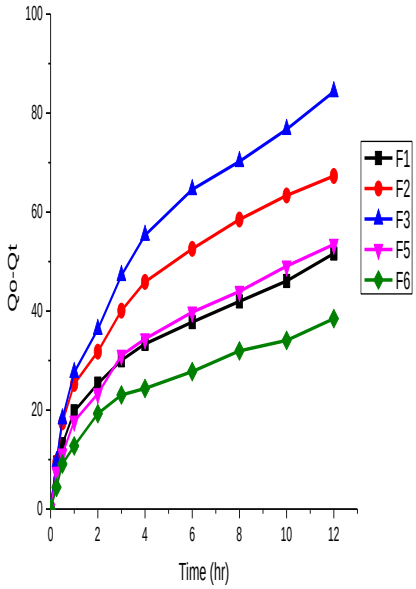

A) Zero order release

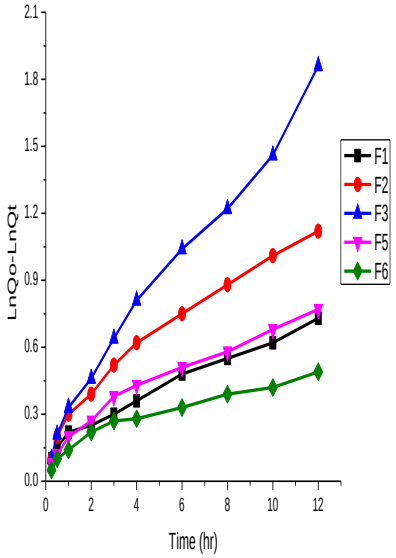

B) First order release

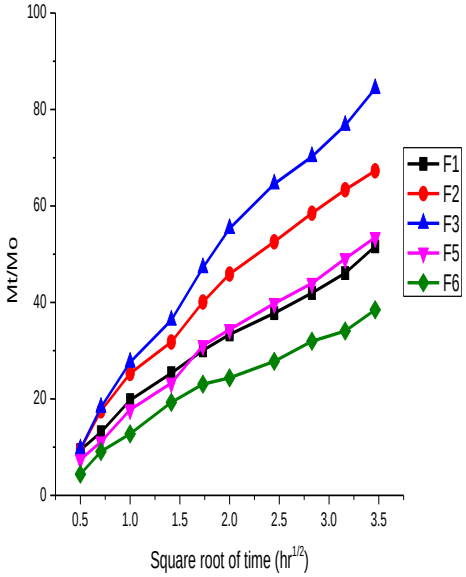

C) Higuchi release model

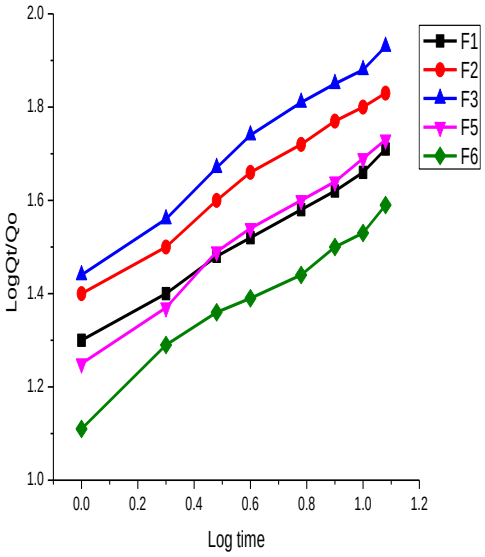

D) Korsmeyer-Peppas release model

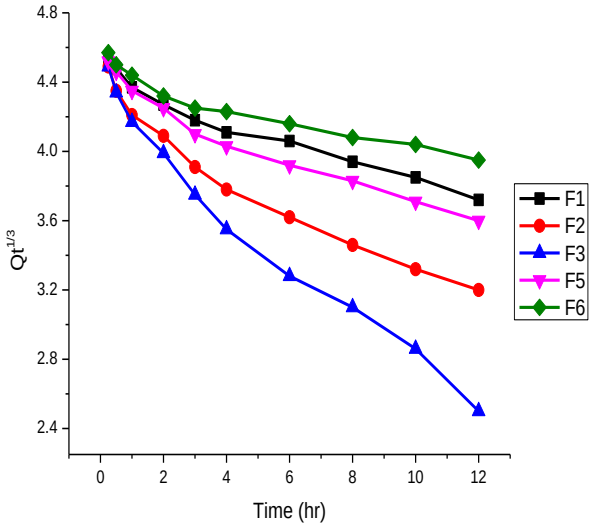

E) Hixson-Crowell model

Figure 16: The release data from the different formulations fitted to various release kinetic models; zero order (A), first order (B), Higuchi (C), Korsmeyer-Peppas (D) and Hixson-Crowell (E) models.

The preference of a certain mechanism was based on the correlation coefficient (R^2) for the parameters studied, where the highest correlation coefficient is preferred for the selection of mechanism of release (Abdel-Rahman *et al*., 2009). In present study, the *in vitro* release profiles of drug from all the formulations could be best expressed by Higuchi's equation, as the plots showed highest linearity (R^2: 0.9862 to 0.9984) as compared to that obtained from zero order, first order, Korsmeyer Peppas and Hixson Crowell model (Table 12). From the results the most probable mechanism of drug release from the matrix system seemed to be diffusion of drug through a porous network created by theophylline already dissolved within the matrix and filled by liquid medium (Chambin *et al*., 2004). This indicates that the release of drug from CLCA matrix is directly proportional to the square root of time i.e., Higuchi model.

The curvilinear nature of cumulative drug release over time (Figure 16A) suggests that none of the formulations follow zero order drug release kinetics, as evidenced by the poor correlation coefficients obtained in all cases. Likewise, the non-linearity of the Hixson-Crowell graph (Figure 16E) and poor correlation coefficient shown in Table 12 suggest that the Hixson-Crowell model is not applicable.

To confirm the mechanism of diffusion, the data were also fit into Korsmeyer- Peppas model (Figure 16D). All the formulations showed linearity (R^2: 0.9768 to 0.9892) with n values ranging from 0.4875 to 0.5417 for F2 to F6 indicating that release mechanism follows non-Fickian diffusion or anomalous release ($0.45 < n < 0.89$). It can be inferred that the release of these formulations were dependent on both drug diffusion and polymer relaxation, suggesting a coupling of two simultaneous mechanisms occurring: diffusion and erosion or the so called anomalous diffusion (Ismail *et al*., 2015). On other hand, the release exponent (n) for F1 value was 0.4426 indicating that, the release mechanism was mainly by diffusion. This was in agreement with other works that postulated a diffusion controlled mechanism when evaluating the drug release mechanism from matrices obtained from hydrophobic polymeric systems (Basak *et al*., 2008).

Table 12: Parameter and statistical estimates of the dissolution data from the different formulations fitted to the different mathematical models.

Models	**Parameters**	**Formulations**				
		F1	**F2**	**F3**	**F5**	**F6**
Zero order	R^2	0.9094	0.8964	0.8998	0.9063	0.8805
	$K(h^{-1})$	3.2334	4.5153	5.7536	3.6601	2.5384
First order	R^2	0.9507	0.9598	0.9760	0.9527	0.9174
	$K(h^{-1})$	0.0464	0.0821	0.1351	0.0554	0.0332
Higuchi	R^2	0.9976	0.9873	0.9862	0.9984	0.9955
	$K(h^{-1/2})$	13.464	18.971	23.498	15.272	10.662
Korsmeyer - Peppas	R^2	0.9839	0.9773	0.9768	0.9892	0.9780
	n	0.4426	0.4875	0.5417	0.5211	0.5109
	$K(h^{-n})$	1.2960	1.3476	1.3862	1.2105	1.1397
Hixson-Crowell	R^2	0.9413	0.9398	0.9592	0.9405	0.9043
	$K(h^{-1/3})$	-0.0631	-0.1035	-0.1474	-0.0739	-0.0471

4. CONCLUSION

Cellulose was successfully extracted from cotton linter (CL). The CLC and CLCA yields were 78.06% and 112.4%, respectively and comparable to those reported elsewhere. The yield and physico-chemical properties of the CLCA depend on the DS. Formation of CLC and CLCA were confirmed by the FTIR spectra. X-ray diffraction showed CLC have high crystallinity index than CLCA while crystallinity index of CLCA DS 2.46 was comparable with CCA. The SEM of CLC showed characteristic morphology that was fibrous while SEM of CLCA revealed it was aggregated. The CLCA with high DS (2.46) exhibited better heat stability than CLC and comparable result with CCA. The CLCA DS 2.46 exhibited a good flowability property suitable for direct compression tableting. The CLCA DS 2.46 also exhibited as a sustained release agent formulations of theophylline. The drug release rate from matrix system depends on the DS and concentration of the CLCA. Increasing the concentration of CLCA resulted a slower release of theophylline from the matrix tablets. The best fit model for the drug release was Higuchi model. Based on the above findings, it may be concluded that the CL is a promising potential source of cellulose and CLCA prepared from CLC can be used in sustained release formulations.

5. SUGGESTIONS FOR FURTHER WORK

Based on these promising results the followings are suggested:

- Characterize the particle size distribution of CLCA.
- Characterize the CLCA in solution, film forming and modify the CLCA into phthalate, butyrate derivatives and study their release properties.
- Correlate the drug release profile obtained *in vitro* with *in vivo* results to confirm that CLCA is able to control and extend the drug release *in vivo* and to establish predictive in vitro-in vivo correlation (IVIVC).

6. REFERENCES

Abdel-Rahman, S.I., Mahrous, G. M. and El-Badry, M.(2009). Preparation and comparative evaluation of sustained release metoclopramide hydrochloride matrix tablets. *Saudi Pharm J* **17**: 283-288.

Abraham, E., Deepa, B., Pothan, L. A., Jacob, M., Thomas, S., Cvelbar, U. and Anandjiwala, R. (2011). Extraction of nanocellulose fibrils from lignocellulosic fibres: A novel approach. *Carbohydr Polym* **86**:1468-1475.

Agustin, M. B., Nakatsubo, F. and Yano, H. (2015). The thermal stability of nanocellulose and its acetates with different degree of polymerization. *Cellulose* **23**:451-464.

Ahuja, D., Kaushik, A. and Singh, M. (2018). Simultaneous extraction of lignin and cellulose nanofibrils from waste jute bags using one pot pre-treatment. *Int J Biol Macromol* **107**:1294-1301.

Akpabio, E. I., Ekong, U. S., Uwah, T. O., Ekpa, E. D., Ubulom, P. M. E., Jacobs, G. E. and Fred, M. E. (2016). Formulation and evaluation of theophylline sustained release tablet using Lasianthera Africana gum. *Niger J Pharm Sci* **5**: 41-48.

Alves, J. A. A., Dos Santos, M. D. L., Morais, C. C., Ascheri, J. L. R., Signini, R., Dos Santos, D. M., Ascheri, D. P. R. (2019). Sorghum straw: Pulping and bleaching process optimization and synthesis of cellulose acetate. *Int J Biol Macromol* **135**: 877-886.

Amaral, H.R., Cipriano, D. F., Santos, M.S., Schettino, M.A., Ferreti, J.V.T., Meirelles, C.S., Pereira, V.S., Cunha, A.G., Emmerich, F.G. and Freitas, J.C.C. (2019). Production of high-purity cellulose, cellulose acetate and cellulose silica composite from babassu coconut shells. *Carbohydr Polym* https://doi.org/10.1016/j.carbpol.2019.01.061.

Amin, F.R., Khalid, H., Zhang, H., Rahman, S., Zhang, R., Liu, G. and Chen, C. (2017). Pretreatment methods of lignocellulosic biomass for anaerobic digestion. AMB Expr **7**: 72.

Araújo, D., Castro, M. C. R., Figueiredo, A., Vilarinho, M. and Machado, A. (2020). Green synthesis of cellulose acetate from corncob: Physicochemical properties and assessment of environmental impacts. *J Clean Prod* **260**: 120865.

Arora, A., Priya, S., Sharma, P., Sharma, S., and Nain, L. (2016). Evaluating biological pretreatment as a feasible methodology for ethanol production from paddy straw. *Biocatal. Agric. Biotechnol* **8**: 66-72.

Asaadi, S., Kakko, T., King, A. W., Kilpeläinen, I., Hummel, M. and Sixta, H. (2018). High-

performance acetylated ioncell-F fibers with low degree of substitution. *ACS Sustain Chem Eng* **6** :9418-9426.

Asman, G. and Akçay, E. (2014). Effect of membrane preparation methods on the release of theophylline through CA membranes at in-vitro condition. *J Macromol Sci* **51**: 326-338.

Ass, B. A. P., Belgacem, M. N. and Frollini, E. (2006). Mercerized linters cellulose: Characterization and acetylation in N,N-dimethylacetamide/lithium chloride. *Carbohydr Polym* **63**:19-29.

ASTM D871- 96., 2010. Standard Test Methods of Testing Cellulose Acetate. West Conshohocken, PA United States 19428-2959.

Azubuike, C. P. and Okhamafe, A. O. (2012). Physicochemical, spectroscopic and thermal properties of microcrystalline cellulose derived from corn cobs. *Int J Recycl Org Waste Agric* **1**: 1-7.

Bahmid, N. A., Syamsu, K .and Maddu, A. (2013). Production of cellulose acetate from oil palm empty fruit bunches cellulose. *Chem Eng Process* **17**: 224-746.

Barbash,V., Yashchenko, O. and Kedrovska, A. (2017). Preparation and properties of nanocellulose from peracetic flax pulp. *J Sci Res Rep* **16**:1-10.

Barbosa, R. F. S., Souza, A.G., Ferreirab, F.F. and Rosa D.S. (2019). Isolation and acetylation of cellulose nanostructures with a homogeneous system. *Carbohydr Polym* **218**:208-217.

Barkalow, D. G., Rowell, R. M.and Young, R. A. (1989). A new approach for the production of cellulose acetate: Acetylation of mechanical pulp with subsequent isolation of cellulose acetate by differential solubility. *J Appl Polym Sci* **37**: 1009-1018.

Barud, H. S., de Araújo Júnior, A. M., Santos, D. B., de Assunção, R. M., Meireles, C. S., Cerqueira, D. A. and Ribeiro, S. J. (2008). Thermal behavior of cellulose acetate produced from homogeneous acetylation of bacterial cellulose. *Thermochimica acta* **471**: 61-69.

Basak, S. C., Kumar, K. S.and Ramalingam, M. (2008). Design and release characteristics of sustained release tablet containing metformin HCl. *Braz J Pharm Sc*i **44**:477-483.

Battisti, R., Hafemann, R., Claumann, C. A., Machado, R.A.F. and Marangoni, C. (2018). Synthesis and characterization of cellulose acetate from royal palm tree agroindustrial waste. *Polym Eng Sci* **59**: 891-898.

Beever, D. K. and Valentine, L. (1958). Studies on the sorption of moisture by polymers. The

cellulose-cellulose acetate system. *J Appl Chem* **8**:103-107.

Beraich, F. Z., Bakasse, M. and Arouch, M. (2016). Synthesis and characterization of cellulose acetate extracted from paper waste. *IRSEC* 785-789. IEEE.

Bezerra, E.B., França, D.C., Morais, D.S., Rosab, M.D., Morais, J.P.S., Araújo, E.M. and Wellen, R.M.R. (2016)**.** Processing and Properties of PCL/Cotton Linter Compounds. *Mater Res http://dx.doi.org/10.1590/1980-5373-MR-2016-0084.*

Bharimalla, A. K.., Deshmukh, S.P., Patil, P.G. and Vigneshwaran, N. (2017).Micro/Nano-fibrillated Cellulose from Cotton Linters as Strength Additive in Unbleached Kraft Paper: Experimental, Semi-empirical, and Mechanistic Studies. *BioResources* **12**: 5682-5696.

Bhattacharya, D., Germinario, L. T. and Winter, W. T. (2008). Isolation, preparation and characterization of cellulose microfibers obtained from bagasse. *Carbohydr Polym* **73**: 371-377.

Bian, J., Peng, F., Peng, X. P., Peng, P., Xu, F. and Sun, R. C. (2012). Acetic acid enhanced purification of crude cellulose from sugarcane bagasse: structural and morphological characterization. *BioResources* **7**: 4626-4639.

Biswas, A., Saha, B.C., Lawton, J.W., Shogren , R.L. and Willett, J.L. (2006). Process for obtaining cellulose acetate from agricultural by-products. *Carbohydr Polym* **64** : 134-137.

Bonet, M., Quijada, C., Muñoz, S. and Cases, F. (2005). The roles of the degree of substitution and the degree of polymerization on the behaviour of cellulose ethers applied as adhesives for artwork conservation. *J Adhes Sci Technol* **19**: 95-108.

Boonterm, M., Sunyadeth, S., Dedpakdee, S., Athichalinthorn, P., Patcharaphun, S., Mungkung, R. and Techapiesancharoenkij, R. (2015). Characterization and comparison of cellulose fiber extraction from rice straw by chemical treatment and thermal steam explosion. *J Clean Prod* **134**: 592-599.

Brandão, L. R., Yoshida, I. V. P., Felisberti, M. I. and do Carmo Gonçalves, M. (2013). Preparation and characterization of cellulose acetate/polysiloxane composites. *Cellulose* **20**: 2791-2802.

Candido, R. G. and Gonçalves, A. R. (2016). Synthesis of cellulose acetate and carboxymethylcellulose from sugarcane straw. *Carbohydr Polym* **152**: 679-686.

Cao, J., Sun, X., Lu, C., Zhou, Z., Zhang, X. and Yuan, G. (2016). Water-soluble cellulose acetate from waste cotton fabrics and the aqueous processing of all-cellulose composites. *Carbohydr Polym* **149**: 60-67.

Cao, L., Luo, G., Tsang, D. C., Chen, H., Zhang, S. and Chen, J. (2018). A novel process for obtaining high quality cellulose acetate from green landscaping waste. *J Clean Prod* **176**: 338-347.

Cao, Y., Zhang, J., He, J., Li, H. and Zhang, Y. (2010). Homogeneous Acetylation of Cellulose at Relatively High Concentrations in an Ionic Liquid. Chinese *J Chem Eng* **18**: 515-522.

Cerqueira, D. A., Rodrigues Filho, G., and da Silva Meireles, C. (2007). Optimization of sugarcane bagasse cellulose acetylation. *Carbohydr Polym* **69**:579-582.

Chambin, O. hampionb, D., Debraya, C., Rochat-Gonthiera, M.H., Le Mesteb, M. and Pourcelot, Y.(2004). Effects of different cellulose derivatives on drug release mechanism studied at a preformulation stage. *J Control Release* **95**: 101-108.

Chauhan, Y. P., Sapkal, R. S., Sapkal, V. S. and Zamre, G. S. (2009). Microcrystalline cellulose from cotton rags (waste from garment and hosiery industries. *Int J Chem Sci* **7**: 681-688

Chen, H., Han, Y. and Xu, J. (2008). Simultaneous saccharification and fermentation of steam exploded wheat straw pretreated with alkaline peroxide. *Process Biochem* **43**: 1462-1466.

Chen, J., Xu, J., Wang, K., Cao, X. and Sun, R. (2016) .Cellulose acetate fibers prepared from different raw materials with rapid synthesis method. *Carbohydr Polym* **137**: 685-692.

Chen, Q., Xiao, S., Shi, S. Q. and Cai, L. (2018). Isolation of cellulose from poplar wood by nitric acid-ethanol treatment and its effect on the quality of films cast from ionic liquid. *BioResources* **13**: 8943-8955.

Chen, X., Yu, J., Zhang, Z. and Lu, C. (2011). Study on structure and thermal stability properties of cellulose fibers from rice straw.*Carbohydr Polym* **85**: 245-250.

Cheng, D., An, X., Zhang, J., Tian, X., He, Z., Wen, Y. and Ni, Y. (2017). Facile preparation of regenerated cellulose film from cotton linter using organic electrolyte solution (OES). *Cellulose* **24**: 1631-1639.

Cheng, H. N., Dowd, M. K., Selling, G. W.and Biswas, A. (2010). Synthesis of cellulose acetate from cotton byproducts. *Carbohydr Polym* **80**: 449-452.

Cherian, B. M., Leão, A. L., De souza, S.F., Thomas, S., Pothan, L.A.and Kottaisamy, M.(2010). Isolation of nanocellulose from pineapple leaf fibres by steam explosion. *Carbohydr Polym* **81**: 720-725.

Dadi, D., Stellmacher,T., Senbeta, F., Van Passel, S. and Azadid, H.(2017). Environmental and Health Impacts of Effluents from Textile Industries in Ethiopia: The Case of Gelan and Dukem, Oromia Regional State. *Environ Monit Assess* **189**: 1-30.

Das, A. M., Ali, A. A. and Hazarika, M. P. (2014). Synthesis and characterization of cellulose acetate from rice husk: Eco-friendly condition. *Carbohydr Polym* **112**: 342-349.

De Freitas, R. R. M., Senna, A. M. and Botaro, V. R. (2017). Influence of degree of substitution on thermal dynamic mechanical and physicochemical properties of cellulose acetate. *Ind Crops Prod* **109**: 452-458.

Deepa, B., Abraham, E., Cherian, B.M., Bismarck, A., Blaker , J.J., Pothan, L.A., Leao, L.A., de Souza, S.F. and Kottaisamy, M. (2011). Structure, morphology and thermal characteristics of banana nano fibers obtained by steam explosion. *Bioresour Technol* **102**: 1988-1997.

Ditzel, F. I., Prestes, E., Carvalho, B. M., Demiate, I. M. and Pinheiro, L. A. (2017). Nanocrystalline cellulose extracted from pine wood and corncob. *Carbohydr Polym* **157**: 1577-1585.

Djuned, F. M., Asadi, M., Ibrahim, M.N.M.and Daud, W.R.W. (2014). Synthesis and characterization of cellulose acetate from TCF oil palm empty fruit bunch pulp. *BioResources* **9**: 4710-4721.

Dong, Z., Hou, X., Sun, F., Zhang, L. and Yang ,Y. (2014). Textile grade long natural cellulose fibers from bark of cotton stalks using steam explosion as a pretreatment. *Cellulose* **21**: 3851-3860.

Draman, S. F. S., Daik, R. and Mohd, N. (2016). Eco-friendly extraction and characterization of cellulose from Lignocellulosoic fiber. *ARPN J Eng Appl Sci* **11**:9591–9595.

Egot, M. P. and Alguno, A. C. (2018). Preparation and Characterization of Cellulose Acetate from Pineapple (Ananas comosus) Leaves. *Key Eng Mater* **772**: 8-12

Eisenhuber, K., Krennhuber, K., Steinmüller, V. and Jäger, A. (2013). Comparison of different pre-treatment methods for separating hemicellulose from straw during lignocellulose bioethanol production. *Energy Procedia* **40**:172-181.

El Nemr, A., Ragab, S. and El Sikaily, A. (2017). Rapid synthesis of cellulose triacetate from cotton cellulose and its effect on specific surface area and particle size distribution. *Iran Polym J* **26**: 261-272.

El Nemr, A., Ragab, S., El Sikaily, A. and Khaled, A. (2015). Synthesis of cellulose triacetate from cotton cellulose by using NIS as a catalyst under mild reaction conditions. *Carbohydr Polym* **130**: 41-48.

Fan, G., Wang, M., Liao, C., Fang,T., Li, J.and Zhou, R. (2013). Isolation of cellulose from rice straw and its conversion into cellulose acetate catalyzed by phosphotungstic acid.*Carbohydr Polym* **94**: 71-76.

Fei, P., Liao, L., Cheng, B.and Song, J. (2017). Quantitative analysis of cellulose acetate with a high degree of substitution by FTIR and its application. *Anal Methods* **9**: 6194-6201.

Fischer, S., Thümmler, K., Volkert, B., Hettrich, K., Schmidt, I. and Fischer, K.(2008). Properties and applications of cellulose acetate. *Macromol Symp* **262**: 89-96.

Galiwango, E., Rahman, N. S. A., Al-Marzouqi, A. H., Abu-Omar, M. M. and Khaleel, A. A. (2019). Isolation and characterization of cellulose and α-cellulose from date palm biomass waste. *Heliyon* **5**: e02937.

Gavilà, L.and Esposito, D. (2017). Cellulose acetate as a convenient intermediate for the preparation of 5-acetoxymethylfurfural from biomass. *Green Chem* **19**: 2496-2500.

Ghareeb, H. O. and Radke, W. (2013). Characterization of cellulose acetates according to DS and molar mass using two-dimensional chromatography. *Carbohydr Polym* **98**:1430-1437.

Gilbert, M. S. and Palle, I. (2013). Cellulose acetate production from Acacia mangium pulp. In *Fourth International Conference on Biology*. *Malaysia* **100**: 118-123.

Gümüskaya, E., Usta, M. and Kirci, H. (2003). The effects of various pulping conditions on crystalline structure of cellulose in cotton linters. *Polym Degrad Stab* **81**: 559-564.

Guerra-Ponce, W. L., Gracia-Vásquez, S. L., González-Barranco, P., Camacho-Mora, I. A., Gracia-Vásquez, Y. A., Orozco-Beltrán, E. and Felton, L. A. (2016). In vitro evaluation of sustained released matrix tablets containing ibuprofen: a model poorly water-soluble drug. *Braz J Pharm Sci* **52**: 751-759.

Guyonnet, T., Brossard, C. and Lefort des Ylouses, D. (1990). Prolongation of theophylline derivative release with cellulose acetate based tablets. *J Pharm Belg* **45**: 111-119.

Haafiz, M. M., Hassan, A., Zakaria, Z., Inuwa, I. M. and Islam, M. S. (2013). Physicochemical characterization of cellulose nanowhiskers extracted from oil palm biomass microcrystalline cellulose. *Mater Lett* **113**: 87-89.

Haleem, N., Arshad, M., Shahid, M. and Tahir, M. A. (2014). Synthesis of carboxymethyl cellulose from waste of cotton ginning industry. *Carbohydr Polym* **113**: 249-255.

Hamad, A. M. A., Ates, S. and Durmaz, E. (2016). Evaluation of the possilities for cellulose derivatives in food products. *J. For* **16**: 383-400.

Haruna, F., Apeji, Y. E., Oparaeche, C., Oyi, A. R. and Gamlen, M. (2020). Compaction and

tableting properties of composite particles of microcrystalline cellulose and crospovidone engineered for direct compression. *Future J Pharm Sci* **6**: 1-9.

Husin, M., Li, A.R., Ramli, N., Romli, A. Z., Hakimi, M. I. and Ilham, Z. (2017). Preparation and characterization of cellulose and microcrystalline cellulose isolated from waste Leucaena leucocephala seeds. *International Journal of Advanced and Applied Sciences* **4**:51-58.

Ibrahim, M. (2002). Preparation of cellulose and cellulose derivative azo compounds. *Cellulose* **9**: 337-349.

Ibrahim, M. M., Agblevor, F. A. and El-Zawawy, W. K. (2010). Isolation and characterization of cellulose and lignin from steam-exploded lignocellulosic biomass. *BioResources* **5**: 397-418.

Ibrahim, M. M. and El-Zawawy,W. K.(2015). Extraction of Cellulose Nanofibers from Cotton Linter and Their Composites. In *Handbook of Polymer Nanocomposites. Processing, Performance and Application* 145-164

Ibrahim, M. M., El-Zawawy, W.K., Juttke, Y., Koschella, K. and Heinze T. (2013). Cellulose and microcrystalline cellulose from rice straw and banana plant waste: preparation and characterization. *Cellulose* **20**: 2403-2416

Ige, P., Swami, B., Patil, T., Pradhan, J., Patil, P., Nerkar, P. and Surana, S. J. (2013). Design and development of sustained release swelling matrix tablets of glipizide for type II diabetes mellitus. *Farmacia* **61**: 883-901.

Ioan, S., Necula, A. M., Stoica, I., Olaru, N., Olaru, L. and Ioanid, G. E. (2009). Surface properties of cellulose acetate. *High Perform Polym* **22**: 598-608.

Ismail, R., Hammad, T. and Madani, F. (2015). Formulation and in vitro evaluation of once-daily methyldopa sustained release matrix tablets. Research J Pharm Tech **8**: 161-166.

Jahan, M. S., Rumee, J. N., Rahman, M. M. and Quaiyyum, A. (2014). Formic acid/acetic acid/water pulping of agricultural wastes. *Cellul Chem Technol* **48**:111-118.

Jandura, P., Riedl, B. and Kokta, B. V. (2000).Thermal degradation behavior of cellulose fibers partially esterified with some long chain organic acids. *Polym Degrad Stab* **70**: 387-394.

Jogunola, O., Eta, V., Hedenström, M., Sundman, O., Salmi, T. and Mikkola, J. P. (2016). Ionic liquid mediated technology for synthesis of cellulose acetates using different co-solvents. *Carbohydr Polym* **135**: 341-348.

Jonasson, S., Bünder, A., Niittylä, T. and Oksman, K. (2019). Isolation and characterization

of cellulose nanofibers from aspen wood using derivatizing and non-derivatizing pretreatments. *Cellulose* **27**: 185-203.

Kale, R. D., Bansal, P. S. and Gorade, V. G. (2017). Extraction of Microcrystalline Cellulose from Cotton Sliver and Its Comparison with Commercial Microcrystalline Cellulose. *J Polym Environ* **26**: 355-364.

Karande, V. S., Bharimalla, A. K., Hadge, G. B., Mhaske, S. T. and Vigneshwaran, N. (2011). Nanofibrillation of cotton fibers by disc refiner and its characterization. *Fiber Polym* **12**: 399.

Khan, M. A., Selvi, S. and Perumal, P. (2019). Formulation development and evaluation of sustained release matrix tablets of Theophylline and Etophylline and study of polymers effect on dissolution rate. *Asian J Pharm Pharmaco* **5**: 101-110.

Khullar, R., Varshney, V. K., Naithani, S., Heinze, T.and Soni, P. L. (2005). Carboxymethylation of cellulosic material (average degree of polymerization 2600) isolated from cotton (Gossypium) linters with respect to degree of substitution and rheological behavior. *J Appl Polym Sci* **96**: 1477-1482.

Klemm, D., Philpp, B., Heinze, T., Heinze, U. and Wagenknecht, W. (1998). Comprehensive cellulose chemistry. *Volume 1: Fundamentals and analytical methods*. Wiley-VCH Verlag GmbH.

Kumar, C. G., Kumar, M. P., Gupta, S., Sunder, M. S., Rao, K. V. M., Jagadeesh, B. and Kamal, A. (2015). Isolation and characterization of cellulose from sweet sorghum bagasse. *Sugar Tech* **17**: 395-403.

Li, J., Zhang, L. P., Peng, F., Bian, J., Yuan, T. Q., Xu, F. and Sun, R. C. (2009). Microwave-assisted solvent-free acetylation of cellulose with acetic anhydride in the presence of iodine as a catalyst. *Molecules* **14**: 3551-3566.

Liu, R., Yu, H. and Huang, Y. (2005). Structure and morphology of cellulose in wheat straw. *Cellulose* **12**: 25-34.

Liu, S. S., Fang, G. G., Deng, Y. J. and Wang, Q. (2011). Preparation of microcrystalline cellulose from cotton linter ethanol pulp. *Adv Mat Res* **295**: 653-658.

Liu, Y., Liu, A., Ibrahim, S. A., Yang, H., and Huang, W. (2018). Isolation and characterization of microcrystalline cellulose from pomelo peel. *Int J Biol Macromol* **111**: 717-721.

Loo, M. M. L., Hashim, R. and Leh, C. P. (2012). Recycling of valueless paper dust to a low grade cellulose acetate: Effect of pretreatments on acetylation. *BioResources* **7**: 1068-1083.

Lu, H., Gui, Y., Zheng, L. and Liu, X. (2013). Morphological, crystalline, thermal and physicochemical properties of cellulose nanocrystals obtained from sweet potato residue. *Food Res Int* **50:** 121-128.

Macuja, J. C. O., Ruedas, L. N. and España, R. C. N. (2015) . Utilization of Cellulose from Luffa cylindrica Fiber as Binder in Acetaminophen Tablets. *Environ Chem* **2015**: doi: 10.1155/2015/243785.

Mansor, A.M., Lim, J.S., Ani, F.N., Hashim,H. and Ho,W.S.(2019). Characteristics of cellulose, hemicellulose and lignin of md2 pineapple biomass. *Chem Eng Trans* **72**: 79-84.

Masareddy, R.S., Kendalakar, P.V.and Belekar,A.M.(2012). Effect of polymers as matrix system in formulation of sustained release theophylline matrix tablet. *Int J Pharm Pharmaceu Sci* **4**: 409-414.

Mihranyan, A., Llagostera, A.P., Karmhag, R., Strømme, M. and Eket, R. (2004) Moisture sorption by cellulose powders of varying crystallinity. *Int J Pharm* **269**:433-442.

Mittal, A., Katahira, R., Himmel, M. E. and Johnson, D. K. (2011). Effects of alkaline or liquid-ammonia treatment on crystalline cellulose: changes in crystalline structure and effects on enzymatic digestibility. *Biotechnol Biofuels* **4**: 1-16.

Mondal, M. I. H. and Alam, A. B. M. F. (2013). Utilization of Cellulosic Wastes in Textile and Garment Industries: Synthesis and Characterization of Cellulose Acetate from Knitted Rag. *J Polym Environ* **21**: 280-285.

Morais, J. P. S., de Freitas Rosa, M., Nascimento, L. D., do Nascimento, D. M. and Cassales, A. R. (2013). Extraction and characterization of nanocellulose structures from raw cotton linter. *Carbohydr. Polym* **91**: 229-235.

Morán, J. I., Alvarez, V., Cyras, V.P. and Vázquez, A. (2008). Extraction of cellulose and preparation of nanocellulose from sisal fibers. *Cellulose* **15**: 149-159.

Mostafa, N. A., Farag, A. A., Abo-dief, H. M. and Tayeb, A. M. (2015). Production of biodegradable plastic from agricultural wastes. *Arab J Chem* **11**: 546-553.

Mzimela, Z. N. T., Linganiso, L. Z., Revaprasadu, N. and Motaung, T. E. (2018). Comparison of cellulose extraction from sugarcane bagasse through Alkali. *Mater Res* **21**: 1-7.

Nabili, A., Fattoum, A., Brochier-Salon, M. C., Bras, J.and Elaloui, E. (2017). Synthesis of cellulose triacetate-I from microfibrillated date seeds cellulose (Phoenix dactylifera L.). *Iran Polym J* **26**: 137-147.

Nadaf, S., Nnamani, P. and Jadhav, N. (2015). Evaluation of Prosopis africana Seed Gum as

an Extended Release Polymer for Tablet Formulation. *AAPS Pharm Sci Tech* **16**: 716-729.

Nagel, K. M. and Peck, G. E. (2003).Investigating the effects of excipients on the powder flow characteristics of theophylline anhydrous powder formulations. *Drug Dev Ind Pharm* **29**: 277-287.

Nazir, M. S.,Wahjoedi, B. A., Yussof, A. W. and Abdullah, M. A. (2013). Eco-friendly extraction and characterization of cellulose from oil palm empty fruit bunches. *BioResources* **8**: 2161-2172.

Nithya, P. D., Brahmani, S., Sriram, A., Krishna, N. P. J., Koteswari, P. and Babu, P. S. (2014). Formulation and Evaluation of Theophylline Controlled Release Matrix Tablets by Using Natural Gums. *Int J Pharm Sci Rev Res* **27**: 183-187.

Neto, W. P.F., Silvério, H.A., Dantas, N.O. and Pasquini, D. (2013). Extraction and characterization of cellulose nanocrystals from agro-industrial residue - Soy hulls. *Ind Crops Prod* **42**: 480-488.

Obeidat, W. M. and Alzoubi, N. M. (2014). Controlled-release cellulose esters matrices for water-soluble diclofenac sodium: Compression and dissolution studies. *Pharmazie* **69**: 96-103.

Ohwoavworhua, F. O., Adelakun, T. A. and Kunle, O. O. (2007). A Comparative Evaluation of the Flow and Compaction Characteristics of a-Cellulose obtained from Waste Paper. *Trop J Pharm Res* **6**: 645-651.

Ojoe, E., Miyauchi, E. M., Kaneko, T. M., Velasco, M. V. R. and Consiglieri, V. O. (2007). Influence of cellulose polymers type on in vitro controlled release tablets containing theophylline. *Braz J Pharm Sci* **43**: 571-579.

Ojoe, E., Miyauchi, E. M., Viviani, T. C. and Consiglieri, V. O. (2005). Formulation and in vitro evaluation of theophylline-Eudragit® sustained-release tablets. *Braz J Pharm Sci* **41**: 377-384.

Oun, A. A. and Rhim, J. W. (2015). Preparation and characterization of sodium carboxymethyl cellulose/cotton linter cellulose nanofibril composite films. *Carbohydr Polym* **127**: 101-109.

Ouyang, X., Chen, L., Zhang, S., Yuan, Q., Wang, W. and Linhardt, L. J. (2018). Effect of simultaneous steam explosion and alkaline depolymerization on corncob lignin and cellulose structure. *Chem Biochem Eng Q* **32**: 177-189.

Pan, X. and Sano, Y. (2005). Fractionation of wheat straw by atmospheric acetic acid process. *Bioresour Technol* **96**: 1256-1263.

Pati, N.B., Gupta,V.R.M.,Velivela, S. and Mayasa, V. (2016). Comparative study of effect of various types of polymers on extended release of tapentadol HCL. *Int J Pharm Technol* **8**: 12762-12775.

Peppas, N. A. (1983). A model of dissolution-controlled solute release from porous drug delivery polymeric systems. *J Biomed Mater Res* **17**:1079-1087.

Phinichka, N. and Kaenthong, S. (2018). Regenerated cellulose from high alpha cellulose pulp of steam-exploded sugarcane bagasse. *J Mater Res Technol* **7**: 55-65.

Poletto, M., Ornaghi Júnior, H. L. and Zattera, A. J. (2014). Native cellulose: Structure, characterization and thermal properties. *Materials* **7**: 6105–6119.

Punčochová, K., Heng, J. Y., Beránek, J. and Štěpánek, F. (2014). Investigation of drug–polymer interaction in solid dispersions by vapour sorption methods. *Int J Pharm* **469**: 159-167.

Punsuvon, V., Vaithanomsat, P. and Iiyama, K. (2008). Simultaneous production of alpha-cellulose and furfural from bagasse by steam explosion pretreatment. *Int J Sci Technol* **2**: 182-191

Quadir, M. A., Chanda, E., Haider, S. S., Reza, M. S. and Datta, B. K. (2005). Evaluation of ethylcellulose as matrices for controlled release drug delivery. *Pak J Pharm Sci* **18**: 29-34.

Quadir, M. A., Rahman, M. S., Karim, M. Z., Akter, S. A., Awkat, M. T. and Reza, M. S. (2003). Evaluation of hydrophobic materials as matrices for controlled-release drug delivery. *Pak J Pharm Sci* **16**: 17-28.

Raatikainen P, Korhonen O, Peltonen S, Paronen P. (2002). Acetylation enhances the tableting properties of starch. *Drug Dev. Ind. Pharm.*, 28: 165-175.

Ragab, T.I.M., Wasfy, A.A.F., Amer,H., EI-Gendi, A.,Abdel-Hady, M.S. and Liebner, F.(2014). Synthesis of cellulose acetate membrane from the Egyptian rice straws. *J. Appl. Sci* **14**: 3424-3435.

Rahman, M., Khan, G.M.A., Uddin, M.H., Abdur Razzaque, S.M. and Shamsul Alam, M. (2016). Chemical Treatments of Cotton Linter Cellulose Fiber for Composite Application. *Am Chem Sci J* **16**: 1-7.

Rajalakshmi, G., Balachandar, R. and Damodharan, N. (2011). Formulation and evaluation of theophylline sustained release matrix tablet. *Der Pharmacia Lettre* **3**:1-7.

Rao, M. R. P., **S**hivpuje, S., Godbole, R. and Shirsath, C. (2016). Design and evaluation of sustained release matrix tablets using sintering technique. *J Pharm Pharm Sc* **8**:115–121.

Ratanakamnuan, U., Atong, D. and Aht-Ong, D. (2012). Cellulose esters from waste cotton fabric via conventional and microwave heating. *Carbohydr Polym* **87**: 84–94.

Reddy, K. O., Maheswari, C. U., Dhlamini, M. S., Mothudi, B. M., Kommula, V. P., Zhang, J.and Rajulu, A. V. (2018). Extraction and characterization of cellulose single fibers from native African Napier grass. *Carbohydr Polym* **188**: 85-91.

Reza, M. S., Quadir, M. A. and Haider, S. S. (2003).Comparative evaluation of plastic, hydrophobic and hydrophilic polymers as matrices for controlled-release drug delivery. *J Pharm Pharm Sc* **6**: 282-291.

Reza, M. S., Quadir, M. A. and Haider, S. S. (2002).Development of theophylline sustained release dosage form based on Kollidon SR. *Pak J Pharm Sci* **15**: 63-70.

Rocha, G. D. M., Gonçalves, A. R., Oliveira, B. R., Olivares, E. G.and Rossell, C. E. V. (2012). Steam explosion pretreatment reproduction and alkaline delignification reactions performed on a pilot scale with sugarcane bagasse for bioethanol production. *Ind Crops Prod* **35**: 274-279.

Rodrigues Filho, G., Almeida, F., Ribeiro, S. D., Tormin, T. F., Muñoz, R. A., Assunção, R. M.and Barud, H. (2015). Controlled release of drugs from cellulose acetate matrices produced from sugarcane bagasse: monitoring by square-wave voltammetry. *Drug Dev Ind Pharm* **42**: 1066-1072.

Rodrigues Filho, G., Monteiro, D. S., da Silva Meireles, C., de Assunção, R. M. N., Cerqueira, D. A., Barud, H. S.and Messadeq,Y. (2008). Synthesis and characterization of cellulose acetate produced from recycled newspaper. *Carbohydr Polym* **73**:74-82.

Roškar, R. and Kmetec, V. (2005). Evaluation of the moisture sorption behaviour of several excipients by BET, GAB and microcalorimetric approaches. *Chem Pharm Bull* **53**: 662-665.

Rosli, N. A., Ahmad, I. and Abdullah, I. (2013). Isolation and characterization of cellulose nanocrystals from agave angustifolia fibre. *BioResources* **8**: 1893–1908.

Sahoo, S. K., Barik, S., Dehury, G., Dhala, S., Kanungo, S., Barik, B. B. and Puhan, K. K. (2011). Evaluation of controlled release theophylline microspheres prepared with cellulose acetate using solvent evaporation method. *Trop J Pharm Res* **10**: 195-201.

Segal, L.G.J.M.A., Creely, J.J., Martin Jr, A.E. and Conrad, C.M. (1959). An empirical method for estimating the degree of crystallinity of native cellulose using the X-ray diffractometer. *Text Res J* **29**: 786–794.

Seo, Y. B., Lee, M. W., Park, D. H.a nd Park, H. J. (2013). Use of a low-energy electron

beam for degree of polymerization control of cotton linter. *Ind Eng Chem Res* **52**: 692-695.

Shaikh, H. M., Pandare, K.V., Nair, G. and Varma, A.J. (2009).Utilization of sugarcane bagasse cellulose for producing cellulose acetates: Novel use of residual hemicellulose as plasticizer. *Carbohydr Polym* **76**: 23-29.

Si, X. P., Zhang, S. J., Chen, Y., Cao, J. H., Cao, Z. X., Luo, K. and Tai, X. Y. (2016). The research development of cellulose acetate fiber and cellulose acetate nanofiber used as filtering materials. *Key Eng Mater* **671**: 279-284.

Singanusong, R., Tochampa, W., Kongbangkerd, T. and Sodchit, C. (2013) Extraction and properties of cellulose from banana peels. *Suranaree J Sci Technol* **21**:201-2013.

Singh, A. V. and Nath, L. K. (2012). Evaluation of acetylated moth bean starch as a carrier for controlled drug delivery. *Int J Biol Macromol* **50**: 362-368.

Singh,S.S., Lim, L.T. and Manickavasagan, A. (2020). Ultrasound-assisted alkali-urea pre-treatment of Miscanthus× giganteus for enhanced extraction of cellulose fiber. *Carbohydr Polym* **247**: 116-758.

Snelders, J., Dornez, E., Benjelloun-Mlayah, B., Huijgen, W. J., de Wild, P. J., Gosselink, R. J. and Courtin, C. M. (2014). Biorefining of wheat straw using an acetic and formic acid based organosolv fractionation process. *Bioresour Technol* **156**: 275-282.

Sonia, A. and Dasan, P. K. (2013). Chemical, morphology and thermal evaluation of cellulose microfibers obtained from Hibiscus sabdariffa. *Carbohydr Polym* **92**: 668-674.

Subhedar, P., Naik, J. B. and Muley, D. N. (2010) . Effect of polymer concentration on sustained release microparticles of metformin hydrochloride prepared by using spray dryer. *Polym Plast Technol Eng* **49**: 267-271.

Sun, J. X., Sun, X. F., Zhao, H. and Sun, R. C. (2004). Isolation and characterization of cellulose from sugarcane bagasse. *Polym Degrad Stab* **84**: 331-339.

Sun, X. F., Sun, R. C., Su, Y. and Sun, J. X. (2004). Comparative study of crude and purified cellulose from wheat straw. *J Agric Food Chem* **52**: 839-847.

Sun, X. F., Xu, F., Sun, R. C., Fowler, P. and Baird, M. S. (2005). Characteristics of degraded cellulose obtained from steam-exploded wheat straw. *Carbohydr Res* **340**: 97-106.

Sun, X., Lu, C., Zhang, W., Tian, D. and Zhang, X. (2013). Acetone-soluble cellulose acetate extracted from waste blended fabrics via ionic liquid catalyzed acetylation. *Carbohydr Polym* **98**: 405-411.

Tarchoun, A. F., Trache, D. and Klapötke, T. M. (2019). Microcrystalline cellulose from Posidonia oceanica brown algae: Extraction and characterization. *Int J Biol Macromol* **138**: 837-845.

Thambiraj, S. and Shankaran, R.D. (2017). Preparation and physicochemical characterization of cellulose nanocrystals from industrial waste cotton. *Appl Surf Sci* **412**: 405-416.

Thomas, L. H., Forsyth, V. T., Šturcová, A., Kennedy, C. J., May, R. P., Altaner, C. M. Jarvis, M. C. (2013). Structure of cellulose microfibrils in primary cell walls from collenchyma. *Plant physiology* **161**: 465-476.

Tomar, M., Kumar, S. A. and Raj, S. A. (2017). Effect of moisture content of exicipient (microcrystalline cellulose) on direct compressible solid dosage forms. *Int J Pharm Sci Res* **8**: 282-288.

Trache, D., Donnot, A., Khimeche, K., Benelmir, R. and Brosse, N. (2014). Physico-chemical properties and thermal stability of microcrystalline cellulose isolated from Alfa fibres. *Carbohydr Polym* **104**: 223-230.

Tutuş, A., Özdemir, A. and Çiçekler, M. (2017). Evaluation of linter cellulose as an alternative raw material for tissue paper production. *Drvna Industrij* **68**: 291-298.

United States Pharmacopoeia 38th ed. National Formulary 33 ed. (USP 38/NF 33) (2015). The United States Pharmacopeial Convention 12601 Twinbrook Parkway, Rockville, MD 20852 .

United States pharmacopeia. 35th revision. National Formulary. 30th ed. (2012). United States Pharmacopeial Convention, Inc., meeting at Washington, D.C.

Vaidya, M. P. and Avachat, A. M. (2011). Investigation of the impact of insoluble diluents on the compression and release properties of matrix based sustained release tablets. *Powder Technol* **214**: 375-381.

Vinayaka, D. L., Guna, V., Madhavi, D., Arpitha, M. and Reddy, N. (2017). Ricinus communis plant residues as a source for natural cellulose fibers potentially exploitable in polymer composites. *Ind Crops Prod* **100**: 126-131.

Vishwanadha, M. K. B., Kumar, B.S., Rajasri, C., Mounika,G., Ramya, D. and Saikrupa.B. (2015). Formulation and evaluation of starch acetate matrix tablets in combination with surfactants for controlled release. *Int J Pharm Sc Res* **6**: 718-722.

Vora, R. S. and Shah, Y. D. (2015). Production of Micro Crystalline Cellulose from Corn Husk and Its Evaluation as pharmaceutical Excipient. *Int J* Sci Res Innov **2**: 69-74.

Wada, M., Heux, L.and Sugiyama, J. (2004). Polymorphism of cellulose I family: reinvestigation of cellulose IVI. *Biomacromolecules* **5**: 1385-1391.

Wagaye, B. T. and Walle, G. A. (2018). Overview of Ethiopian Textile Industry. *J text polym* **6**: 2012-2015.

Wang, H., Wen, X., Zhang, X. and Liu, C. (2017). Acetylation of microcrystalline cellulose by transesterification in AmimCl/DMSO cosolvent system. *Molecules* **22**: 1419.

Wan, S., Sun, Y., Qi, X. and Tan, F. (2012). Improved bioavailability of poorly water-soluble drug curcumin in cellulose acetate solid dispersion. *AAPS pharm Sci Tech* **13**: 159-166.

Yang, W., Cheng, T., Feng, Y., Qu, J., He, H. and Yu, X. (2017). Isolating cellulose nanofibers from steam-explosion pretreated corncobs using mild mechanochemical treatments. *BioResources* **12**: 9183-9197.

Yang, W., Feng, Y., He, H.and Yang, Z. (2018). Environmentally-friendly extraction of cellulose nanofibers from steam-explosion pretreated sugar beet pulp. *Materials* **11**: 1160.

Zhang, L., Xie, W., Zhao, X., Liu, Y. and Gao, W. (2009). Study on the morphology, crystalline structure and thermal properties of yellow ginger starch acetates with different degrees of substitution. *Thermochim Acta* **495**: 57-62.

Zhang, M., Qi, W., Liu, R., Su, R., Wu, S. and He, Z. (2010). Fractionating lignocellulose by formic acid: characterization of major components. *Biomass Bioenergy* **34**: 525-532.

Zhou, X., Lin, X., White, K. L., Lin, S., Wu, H., Cao, S., Huang , L. and Chen, L. (2016). Effect of the degree of substitution on the hydrophobicity of acetylated cellulose for production of liquid marbles. *Cellulose* **23**: 811-821.

Zuliahani, A., Nurul Nadhirah, R., Rozyanty, A. R., Nawawi, W. I. and Nor Hanani, A.B. (2016). Crystallinity, Tapping and Bulk Density of Microcrystalline Cellulose (MCC) Isolated from Rice Husk (RH). *Appl Mech Mater* **835**: 272-276.